MATHEMATICAL ENGINEERING
TECHNICAL REPORTS

Truss Topology Optimization with a Limited Number of Different Cross-Sections: A Mixed-Integer Second-Order Cone Programming Approach

Yoshihiro KANNO

METR 2014–30 November 2014

DEPARTMENT OF MATHEMATICAL INFORMATICS
GRADUATE SCHOOL OF INFORMATION SCIENCE AND TECHNOLOGY
THE UNIVERSITY OF TOKYO
BUNKYO-KU, TOKYO 113-8656, JAPAN

WWW page: http://www.keisu.t.u-tokyo.ac.jp/research/techrep/index.html

Truss Topology Optimization with a Limited Number of Different Cross-Sections: A Mixed-Integer Second-Order Cone Programming Approach

Yoshihiro Kanno †

Department of Mathematical Informatics,
University of Tokyo, Tokyo 113-8656, Japan

Abstract

In deign practice it is often that the structural components are selected from among easily available discrete candidates and a number of different candidates used in a structure is restricted to be small. Presented in this paper is a truss topology optimization method for finding the minimum compliance design in which only a limited number of different cross-section sizes are employed. The member cross-sectional areas are considered either discrete design variables that can take only predetermined values or continuous design variables. In both cases it is shown that the compliance minimization problem can be formulated as a mixed-integer second-order cone programming problem. The global optimal solution of this optimization problem is then computed by using an existing solver based on a branch-and-cut algorithm. Numerical experiments are performed to show that the proposed approach is applicable to moderately large-scale problems.

Keywords

Topology optimization; global optimization; mixed-integer programming; second-order cone programming; optimal standardization.

1 Introduction

This paper attempts to shed new light on a classical problem in the truss topology optimization. We consider the minimization problem of the compliance under the volume constraint. Within the framework of the ground structure approach, the member cross-sectional areas are considered the continuous design variables. Then we deal with an optimization problem for finding the stiffest truss design that consists of only a limited number of different member sizes (cross-sectional areas).

It is known that the minimum compliance problem of trusses with continuous design variables can be recast as a *second-order cone programming* (SOCP) problem. This SOCP problem plays a fundamental role in formulating the optimization problems proposed in this paper. Based upon the minimum principle of complementary energy for the equilibrium analysis, the SOCP problem is formulated in terms of the member cross-sectional areas, axial forces, and the complementary strain energies. The second-order cone constraints stem from the definition of the complementary strain

†Address: Department of Mathematical Informatics, Graduate School of Information Science and Technology, University of Tokyo, Tokyo 113-8656, Japan. E-mail: kanno@mist.i.u-tokyo.ac.jp. Phone: +81-3-5841-6906. Fax: +81-3-5841-6886.

energy stored in each member. SOCP is a class of convex optimization and its optimal solution can be computed efficiently with a primal-dual interior-point method [2, 4].

Formulations based upon the minimum principle of complementary energy have sometimes been used in studies of compliance minimization problems of continua [3, 9, 21]. This type of formulation for trusses is due to Bendsøe *et al.* [8]. There, the problem was not recast as an SOCP problem. Moreover, one should use positive lower bounds for the member cross-sectional areas, because the complementary strain energy is inversely proportional to the member cross-sectional area. The SOCP formulation, however, does not require the positive lower bound; indeed, the cross-sectional areas are allowed to become equal to zeros in the optimization process. This SOCP formulation, briefly recalled in section 2.2 of this paper, can be found in Makrodimopoulos *et al.* [26]. The dual problem of this SOCP problem may be regarded as a type of minimum compliance problems based upon the minimum principle of total potential energy. A problem of this type can be found in Jarre *et al.* [20]; see also Ben-Tal and Bendsøe [6].

Optimization with the continuous design variables often results in a truss design which is not practical in several respects. The member cross-sectional areas of the optimal design can possibly take all different values, which is not acceptable for commercial and manufacturability reasons. Also, existence of too thin members is not accepted. Therefore, formulations and algorithms for truss optimization with discrete design variables have been studied extensively; see, e.g., [25] for a survey on early contributions. One approach is to make use of the continuous optimal solution as a basis for a discrete design. A simple method is rounding each cross-sectional area of the continuous optimal solution to a near discrete predetermined candidate value. Several rounding strategies have been proposed in, e.g., [16, 17, 31, 32]. In general optimality and/or feasibility are not guaranteed by such a heuristic method. Another approach is to directly deal with a discrete optimization problem based upon *mixed-integer programming* (MIP) methodology. Particularly, *mixed-integer nonlinear programming* (MINLP) formulations have been studied extensively. Early contributions include the algorithms in [12, 28], which solve a sequence of subproblems that are formulated as *mixed-integer linear programming* (MILP) problems. Schmit and Fleury [32] proposed a dual method to deal with a separable approximation of the original MINLP problem. The methods [12, 28, 32] cited above do not guarantee global optimality. For truss optimization problems with discrete cross-sectional areas, MINLP approaches with the guaranteed global optimality have been developed in [1, 13, 34]. Also, Stolpe and Kawamoto [35] proposed an MINLP approach considering geometrical nonlinearity in order to solve a design problem of link mechanisms. An outer approximation method for MINLP has been proposed in [23] for solving a certain class of topology optimization problems. An MILP formulation for truss topology optimization under the stress constraints is due to Rasmussen and Stolpe [29]. This formulation, briefly recalled in section 2.3 of this paper, follows naturally from the MILP formulation developed in [36] for continuum-based topology optimization under the stress constraints. Bollapragada *et al.* [11] proposed a mixed-logical linear programming approach for truss optimization under the displacement constraints. This approach uses a small positive lower bound for the member cross-sectional areas and considers the elongation constraints for the all members included in the ground structure. Therefore, truss topology is not optimized in a strict sense. It should be clear that, in the literature [1, 11–13, 16, 17, 28, 29, 31, 32, 34] cited above, the set of discrete values available for design variables is predetermined.

MINLP has also been applied to truss optimization with continuous member cross-sectional areas. The methods in [27, 30], however, do not guarantee global optimality.

If a number of available discrete sizes and/or a number of members in a ground structure are large, then it is usual that global optimization methods based upon enumeration of solutions consume a lot of time. On the other hand, if the available discrete sizes are closely spaced, it sometimes happens that a solution found by a method without guaranteed global optimality, e.g., rounding the continuous optimal solution, is near optimal. However, the obtained discrete design may use a large number of different available sizes. As pointed out by Templeman [37], such a design has several disadvantages from a practical point of view and a truss design that uses only a small number of different sizes would be much more practical. If a quite small number of available discrete sizes is postulated, then the optimal solution could be expected to use only a limited number of different sizes. For such a problem, rounding the continuous optimal solution is often far less efficient [37] and a global optimization approach could be applicable, provided that the number of design variables is moderately small. However, the optimal solution highly depends on the set of predetermined available discrete sizes; this dependence is concretely shown through the numerical experiments presented in section 5.1. Therefore, it is not clear how one can choose values of widely-spaced sizes, in advance, to assure high quality of mechanical performance of the discrete optimal solution.

This paper develops a *mixed-integer second-order cone programming* (MISOCP) approach that attempts to solve these issues. Namely, to find a truss design that has high performance as far as possible and uses only a small number of different sizes, we directly address an upper bound constraint for the number of different cross-sectional areas. The member cross-sectional areas can be considered either continuous design variables or to be selected among (closely-spaced, if necessary) predetermined available sizes. MISOCP[1] is a class of optimization problems in the form of

$$\begin{aligned}
\min \quad & \boldsymbol{f}^\top \boldsymbol{x} + \boldsymbol{r}^\top \boldsymbol{y} && \text{(1a)}\\
\text{s.t.} \quad & \|A_i \boldsymbol{x} + G_i \boldsymbol{y} + \boldsymbol{b}_i\| \le \boldsymbol{d}_i^\top \boldsymbol{x} + \boldsymbol{e}_i^\top \boldsymbol{y} + h_i, \quad i = 1, \ldots, k, && \text{(1b)}\\
& \boldsymbol{x} \in \{0,1\}^n, && \text{(1c)}\\
& \boldsymbol{y} \in \mathbb{R}^p. && \text{(1d)}
\end{aligned}$$

Here, $\boldsymbol{x}$ and $\boldsymbol{y}$ are variables to be optimized, $A_i \in \mathbb{R}^{m_i \times n}$ and $G_i \in \mathbb{R}^{m_i \times p}$ $(i = 1, \ldots, k)$ are constant matrices, $\boldsymbol{f} \in \mathbb{R}^n$, $\boldsymbol{r} \in \mathbb{R}^p$, $\boldsymbol{b}_i \in \mathbb{R}^{m_i}$, $\boldsymbol{d}_i \in \mathbb{R}^n$, and $\boldsymbol{e}_i \in \mathbb{R}^p$ $(i = 1, \ldots, k)$ are constant vectors, $h_i \in \mathbb{R}$ $(i = 1, \ldots, k)$ are constant scalars, and $\|A_i \boldsymbol{x} + G_i \boldsymbol{y} + \boldsymbol{b}_i\|$ denotes the standard Euclidean norm of $A_i \boldsymbol{x} + G_i \boldsymbol{y} + \boldsymbol{b}_i$, i.e., $\|\boldsymbol{v}\| = (\boldsymbol{v}^\top \boldsymbol{v})^{1/2}$ for vector $\boldsymbol{v}$. If we replace binary constraints, (1c), with linear constraints, $0 \le x_j \le 1$ $(j = 1, \ldots, n)$, then the resulting relaxation problem is SOCP. By virtue of this property, MISOCP (1) can be solved globally by using, e.g., a branch-and-bound method; see, e.g., [5, 14, 38] for more account. For solving MISOCP globally, several well-developed software packages, e.g., CPLEX [19] and Gurobi Optimizer [18], are available. In the field of structural optimization, MISOCP has recently been applied to a damper placement optimization problem for supplemental damping of a building structure [22]. The MISOCP formulation proposed in this paper is based upon the SOCP formulation for the continuous compliance optimization of trusses

[1] Also called mixed-integer conic quadratic programming.

mentioned above. Indeed, the former can be viewed as a natural extension of the latter in the sense that the continuous relaxation of the former coincides with the latter.

Recently, Lavan and Amir [24] have proposed an MINLP formulation for a closely related structural optimization problem. They considered an optimization problem of the damping coefficients of viscous dampers that are used for seismic retrofitting of a building and addressed the upper bound constraint for the number of different damper sizes. Let x_e denote the damping coefficient of damper e and suppose that the upper bound is two. By making use of binary variables s_{e1} and s_{e2}, this constraint can be written as

$$x_e = s_{e1}[(1 - s_{e2})y_1 + s_{e2}y_2], \quad \forall e, \tag{2a}$$

$$s_{e1}, s_{e2} \in \{0, 1\} \quad \forall e, \tag{2b}$$

where y_1, $y_2 \in \mathbb{R}$ are additional variables representing the adopted values of the damping coefficients. In the problem setting considered in this paper, x_e is regarded as the cross-sectional area of truss member e. However, due to nonconvexity of constraint (2a), it seems to be difficult to develop an algorithm with guaranteed global optimality; formulation (2) yields an MINLP problem, the continuous relaxation of which is a nonconvex optimization problem. Formulation (2) is originated from the one for multi-phase material topology optimization of continua [15, 33]. By using the idea there, the formulation can be extended to any value of the upper bound; for instance, if the upper bound for different design variables is three, then we obtain

$$x_e = s_{e1}[(1 - s_{e2})y_1 + s_{e2}(1 - s_{e3})y_2 + s_{e2}s_{e3}y_3], \quad \forall e,$$

$$s_{e1}, s_{e2}, s_{e3} \in \{0, 1\}, \quad \forall e.$$

This case includes a higher-order term, $s_{e1}s_{e2}s_{e3}y_3$, than (2). Thus difficulty of the optimization problem depends on the upper bound for different design variables. In contrast, with the formulation developed in this paper, the compliance optimization problem can be formulated as MISOCP irrespective of the upper bound. Again, a remarkable advantage of the MISOCP approach is guaranteed convergence to a global optimal solution and no need for developing algorithms specialized for specific optimization problems.

The paper is organized as follows. Section 2 recalls the two existing formulations, the SOCP formulation of the compliance optimization with continuous design variables and the MILP formulation of that with discrete design variables. Section 3 presents the MISOCP formulation for the compliance optimization with the upper bound constraint on the number of different member cross-sectional areas. Section 4 explores some practical constraints on the member cross-sectional areas that can be considered within the framework of MISOCP. Section 5 presents numerical experiments. Conclusions are drawn in section 6.

A few words regarding notation. All vectors are assumed to be column vectors. The $(m + n)$-dimensional column vector $(\boldsymbol{z}^\top, \boldsymbol{x}^\top)^\top$ consisting of $\boldsymbol{z} \in \mathbb{R}^m$ and $\boldsymbol{x} \in \mathbb{R}^n$ is often written simply as $(\boldsymbol{z}, \boldsymbol{x})$. For a finite set S, we use $|S|$ to denote the cardinality of S, i.e., the number of (different) elements in S. For instance, if $s_1 = s_2 = 1$, $s_3 = 3$, and $s_4 = s_5 = 4$, then $|\{s_i \mid i = 1, \ldots, 5\}| = 3$. For a, $b \in \mathbb{R}$ with $a < b$, we denote by $[a, b]$ and $]a, b[$ the closed and open intervals between a and

b, respectively, i.e.,

$$[a, b] = \{x \in \mathbb{R} \mid a \leq x \leq b\},$$
$$]a, b[= \{x \in \mathbb{R} \mid a < x < b\}.$$

For $x \in \mathbb{R}$, we use $\lfloor x \rfloor$ to denote the largest integer that is not greater than x.

2 Review of exiting formulations for compliance optimization

This section summarizes fundamentals of the compliance optimization of truss structures. Section 2.1 defines this optimization problem. Section 2.2 recalls its SOCP formulation, which serves as a basis for the MISOCP formulations developed in sections 3 and 4. As another relevant problem, section 2.3 recalls the MILP formulation for the problem in which each cross-sectional area is chosen among finitely many predetermined available values.

2.1 Compliance minimization problem

Following the conventional ground structure approach, consider a truss consisting of many candidate members connected by nodes. Throughout the paper we assume small deformation and linear elasticity. Let m and d denote the number of members and the number of degrees of freedom of the displacements, respectively. We use x_e to denote the cross-sectional area of member e and write $\boldsymbol{x} = (x_1, \ldots, x_m)^\top$ which is the vector of design variables to be optimized.

Let $\boldsymbol{u} \in \mathbb{R}^d$ and $c_e \in \mathbb{R}$ denote the vector of displacements and the elongation of member e, respectively. The compatibility relation between $\boldsymbol{u}$ and c_e is written as

$$c_e = \boldsymbol{b}_e^\top \boldsymbol{u}, \quad e = 1, \ldots, m, \tag{3}$$

where $\boldsymbol{b}_e \in \mathbb{R}^d$ is a constant vector. The stiffness matrix, denoted $K(\boldsymbol{x}) \in \mathbb{R}^{d \times d}$, is given by

$$K(\boldsymbol{x}) = \sum_{e=1}^{m} \frac{E x_e}{l_e} \boldsymbol{b}_e \boldsymbol{b}_e^\top, \tag{4}$$

where l_e is the undeformed length of member e and E is Young's modulus. Let $\boldsymbol{f} \in \mathbb{R}^d$ denote the vector of external forces. The compliance, denoted $\pi(\boldsymbol{x}) \in \mathbb{R} \cup \{+\infty\}$, is then defined by

$$\pi(\boldsymbol{x}) = \sup\{2\boldsymbol{f}^\top \boldsymbol{u} - \boldsymbol{u}^\top K(\boldsymbol{x}) \boldsymbol{u} \mid \boldsymbol{u} \in \mathbb{R}^d\}. \tag{5}$$

Let $\bar{V}$ and $x^{\max}$ denote the specified upper bounds for the structural volume and for the member cross-sectional area, respectively. The compliance minimization problem is formulated as

$$\min \quad \pi(\boldsymbol{x}) \tag{6a}$$
$$\text{s.t.} \quad \sum_{e=1}^{m} l_e x_e \leq \bar{V}, \tag{6b}$$
$$0 \leq x_e \leq x^{\max}, \quad e = 1, \ldots, m. \tag{6c}$$

2.2 SOCP formulation for continuous design variables

It is known that problem (6) can be recast as an SOCP problem; see, e.g., Makrodimopoulos *et al.* [26]. The SOCP problem is formulated in variables x_e, w_e, and q_e ($e = 1, \ldots, m$) as

$$\begin{aligned}
\min \quad & 2\sum_{e=1}^{m} w_e && \text{(7a)}\\
\text{s.t.} \quad & w_e + x_e \geq \left\| \begin{bmatrix} w_e - x_e \\ \sqrt{2l_e/E}\, q_e \end{bmatrix} \right\|, \quad e = 1, \ldots, m, && \text{(7b)}\\
& \sum_{e=1}^{m} q_e \boldsymbol{b}_e = \boldsymbol{f}, && \text{(7c)}\\
& \sum_{e=1}^{m} l_e x_e \leq \bar{V}, && \text{(7d)}\\
& 0 \leq x_e \leq x^{\max}, \qquad e = 1, \ldots, m. && \text{(7e)}
\end{aligned}$$

Here, for each $e = 1, \ldots, m$, the inequality constraint in (7b) is a second-order cone constraint in terms of $w_e + x_e$, $w_e - x_e$, and $\sqrt{2l_e/E}\, q_e$. Variables w_e and q_e correspond to the complementary strain energy and the axial force, respectively, of member e.

Details of derivation of problem (7) appear in appendix A.

2.3 MILP formulation for discrete design variables

We next suppose that the cross-sectional area of each member is to be chosen among some predetermined candidate values. That is, we add the constraint

$$x_e \in \{0, \bar{\xi}_1, \ldots, \bar{\xi}_p\}, \quad e = 1, \ldots, m. \tag{8}$$

to problem (6), where $\bar{\xi}_1, \ldots, \bar{\xi}_p$ are predetermined positive constants.

It is known that this optimization problem can be reformulated as an MILP problem; see e.g., [29]. For member e, we introduce binary variables, $\tau_{e1}, \ldots, \tau_{ep}$, to indicate the adopted candidate value for x_e, in a manner such that $\tau_{ei} = 1$ means $x_e = \bar{\xi}_i$. Constraint (8) can be rewritten as

$$\begin{aligned}
x_e &= \sum_{i=1}^{p} \bar{\xi}_i \tau_{ei},\\
\sum_{i=1}^{p} \tau_{ei} &\leq 1,\\
\tau_{ei} &\in \{0, 1\}, \quad i = 1, \ldots, p.
\end{aligned}$$

By using this expression, the optimization problem can be reformulated as the following MILP

problem:

$$\begin{aligned}
\min \quad & \boldsymbol{f}^\top \boldsymbol{u} && && \text{(9a)}\\
\text{s.t.} \quad & \sum_{e=1}^{m}\sum_{i=1}^{p} \frac{E\bar{\xi}_i}{l_e}\chi_{ei}\boldsymbol{b}_e = \boldsymbol{f}, && && \text{(9b)}\\
& |\chi_{ei} - \boldsymbol{b}_e^\top \boldsymbol{u}| \le M(1-\tau_{ei}), && e=1,\dots,m;\ i=1,\dots,p, && \text{(9c)}\\
& |\chi_{ei}| \le M\tau_{ei}, && e=1,\dots,m;\ i=1,\dots,p, && \text{(9d)}\\
& \sum_{e=1}^{m} l_e\Big(\sum_{i=1}^{p}\bar{\xi}_i\tau_{ei}\Big) \le \bar{V}, && && \text{(9e)}\\
& \sum_{i=1}^{p}\tau_{ei} \le 1, && e=1,\dots,m, && \text{(9f)}\\
& \tau_{ei} \in \{0,1\}, && e=1,\dots,m;\ i=1,\dots,p. && \text{(9g)}
\end{aligned}$$

Here, $M \gg 0$ is a sufficiently large constant. Variables to be optimized are $\boldsymbol{u}$, χ_{ei}, and τ_{ei} ($e = 1,\dots,m;\ i = 1,\dots,p$).

3 Standardization constraints

This section presents MISOCP formulations for truss topology optimization with the upper bound constraint for the number of different cross-sectional areas. Section 3.1 deals with a simple case in which a truss should consist of members with uniform cross-sectional areas. This result is generalized in section 3.2 for the constraint that n different cross-sectional areas can be used in a truss design. Section 3.3 shows a scale-free property of the optimization problems in sections 3.1 and 3.2.

3.1 Uniformity constraint on member cross-sections

In this section we attempt to find a truss design that minimizes the compliance when the truss consists of members that have the same cross-sectional areas. The optimal value of the unified cross-sectional area is explored from a set $[0, x^{\max}]$, where $x^{\max}$ is a specified upper bound. This topology optimization problem essentially consists of the following two factors:

- Determine whether each member has a positive cross-sectional area or vanishes;
- Determine the common value of cross-sectional areas for existing members.

The formulation developed below make use of m binary design variables for the former decision and one continuous design variable for the latter decision.

The condition under consideration is satisfied if and only if there exists $y \in [0, x^{\max}]$ such that $x_1,\dots,x_m$ satisfy

$$x_e \in \{0, y\}. \tag{10}$$

We rewrite (10) with making use of binary variables $t_e \in \{0,1\}$ ($e = 1,\dots,m$) that indicate existing members. Namely, $t_e = 0$ means that member e vanishes, i.e., $x_e = 0$, while $t_e = 1$ means member

e exists, i.e., $x_e > 0$. Then condition (10) can be expressed as

$$x_e = \begin{cases} y & \text{if } t_e = 1, \\ 0 & \text{if } t_e = 0. \end{cases} \tag{11}$$

In conjunction with $x_e \in [0, x^{\max}]$ and $y \in [0, x^{\max}]$, we can restate (11) as

$$\begin{aligned} 0 \le x_e &\le x^{\max} t_e, \\ |x_e - y| &\le x^{\max}(1 - t_e), \end{aligned}$$

which are linear inequality constraints in terms of x_e, y, and t_e.

The observation above can be stated formally as follows.

Proposition 3.1. *Suppose* $0 \le y \le x^{\max}$. *Then* x_e *satisfies*

$$x_e \in \{0, y\} \tag{12}$$

if and only if there exist t_e *satisfying*

$$0 \le x_e \le x^{\max} t_e, \tag{13a}$$

$$|x_e - y| \le x^{\max}(1 - t_e), \tag{13b}$$

$$t_e \in \{0, 1\}. \tag{13c}$$

Proof. Suppose $t_e = 1$ in (13c). Then (13a) and (13b) are reduced to

$$\begin{aligned} 0 \le x_e &\le x^{\max}, \\ |x_e - y| &\le 0, \end{aligned}$$

which imply $x_e = y$ and hence (12) is satisfied. Conversely, if $x_e = y$, then $t_e = 1$ satisfies (13). Alternatively, suppose $t_e = 0$ in (13c). Then (13a) and (13b) are reduced to

$$\begin{aligned} 0 \le x_e &\le 0, \\ |x_e - y| &\le x^{\max}, \end{aligned}$$

which are equivalent to $x_e = 0$ and $|y| \le x^{\max}$ and hence (12) is satisfied. Conversely, if $x_e = 0$, then $t_e = 0$ satisfies (13). □

Remark 3.2. Since too thin members are not allowed to present from a practical point of view, the specified lower bound for the cross-sectional areas of existing members, i.e., the slenderness constraint, are often considered. Let $x^{\min}$ (> 0) denote the specified lower bound. With the slenderness constraint the member cross-sectional area is now required to satisfy

$$x_e \in \{0\} \cup [x^{\min}, x^{\max}].$$

The result in Proposition 3.1 can be extended to this case by replacing (13a) with

$$x^{\min} t_e \le x_e \le x^{\max} t_e$$

for each $e = 1, \ldots, m$. ■

We are now in position to present an MISOCP formulation for truss optimization with uniform member cross-sectional areas. Recall that the conventional compliance optimization problem has been formulated as SOCP problem (7). Application of Proposition 3.1 yields the following problem:

$$\begin{aligned}
\min \quad & 2\sum_{e=1}^{m} w_e && && \text{(14a)}\\
\text{s.t.} \quad & w_e + x_e \geq \left\| \begin{bmatrix} w_e - x_e \\ \sqrt{2l_e/E}\, q_e \end{bmatrix} \right\|, && e = 1, \ldots, m, && \text{(14b)}\\
& \sum_{e=1}^{m} q_e \boldsymbol{b}_e = \boldsymbol{f}, && && \text{(14c)}\\
& \sum_{e=1}^{m} l_e x_e \leq \bar{V}, && && \text{(14d)}\\
& 0 \leq x_e \leq x^{\max} t_e, && e = 1, \ldots, m, && \text{(14e)}\\
& |x_e - y| \leq x^{\max}(1 - t_e), && e = 1, \ldots, m, && \text{(14f)}\\
& t_e \in \{0, 1\}, && e = 1, \ldots, m. && \text{(14g)}
\end{aligned}$$

In this problem, x_e, w_e, q_e ($e = 1, \ldots, m$) and y are continuous design variables and t_e ($e = 1, \ldots, m$) are binary design variables. At the optimal solution, y becomes equal to the unified value of the cross-sectional areas of the existing members. Inequalities in (14b) are second-order cone constraints. Constraints (14c), (14d), and (14e) are linear constrains. Inequalities in (14f) can be treated as second-order cone constraints in the two-dimensional space or, alternatively, can be reduced to linear inequality constraints as

$$-x^{\max}(1 - t_e) \leq x_e - y \leq x^{\max}(1 - t_e).$$

Thus all the constraints other than (14g) are in the forms of linear or second-order cone constraints. Also, the objective function is a linear function. Therefore, problem (14) is an MISOCP problem.

Remark 3.3. Problem (7) corresponds to a continuous relaxation of problem (14). To see this, we show that for any $x_1, \ldots, x_m \in [0, x^{\max}]$ there exist $t_1, \ldots, t_m \in [0, 1]$ and y satisfying (14e) and (14f). Indeed, $t_e = x_e/x^{\max}$ ($e = 1, \ldots, m$) and $y = x^{\max}$ satisfy these conditions. ■

3.2 Upper bound constraint on number of different cross-sections

Suppose that we adopt, not necessarily unique, but a limited number of different values for the design variables. Let n denote the specified upper bound for the number of different cross-sectional areas. Then the constraint restricting the variation of cross-sectional areas can be written as

$$|\{x_e \mid e = 1, \ldots, m\} \setminus \{0\}| \leq n. \tag{15}$$

It is worth noting that (15) with $n = 1$ corresponds to the constraint studied in section 3.1.

Like the discussion in section 3.1, we formulate this condition as a system of linear inequalities by making use of some 0-1 variables. The key to this reformulation is that the condition under consideration is satisfied if and only if there exist $y_1, \ldots, y_n \in [0, x^{\max}]$ such that $x_1, \ldots, x_m$ satisfy

$$x_e \in \{0, y_1, \ldots, y_n\}. \tag{16}$$

For member e, we introduce binary variables $s_{e1}, \ldots, s_{en} \in \{0, 1\}$ to represent the relations between x_e and $y_1, \ldots, y_n$. Let $s_{ej} = 1$ imply that cross-sectional area y_j is used for member e, i.e.,

$$x_e = y_j \quad \Leftarrow \quad s_{ej} = 1. \tag{17}$$

Also, $s_{e1} = \cdots = s_{en} = 0$ implies that member e is removed, i.e.,

$$x_e = 0 \quad \Leftarrow \quad s_{e1} = \cdots = s_{en} = 0. \tag{18}$$

Without loss of generality we can assume that at most one of $s_{e1}, \ldots, s_{en}$ becomes 1, i.e.,

$$\sum_{j=1}^{n} s_{ej} \leq 1$$

Then, in conjunction with $x_e \in [0, x^{\max}]$ and $y_j \in [0, x^{\max}]$, condition (17) can be rewritten as

$$|x_e - y_j| \leq x^{\max}(1 - s_{ej}),$$

while condition (18) can be rewritten as

$$0 \leq x_e \leq x^{\max} \sum_{j=1}^{n} s_{ej}.$$

The reformulation sketched above can be stated formally as follows.

Proposition 3.4. *Suppose* $0 \leq y_j \leq x^{\max}$ $(j = 1, \ldots, n)$. *Then* x_e *satisfies*

$$x_e \in \{0, y_1, \ldots, y_n\}, \tag{19}$$

if and only if there exist t_e *and* $s_{e1}, \ldots, s_{en}$ *satisfying*

$$0 \leq x_e \leq x^{\max} t_e, \tag{20a}$$

$$|x_e - y_j| \leq x^{\max}(1 - s_{ej}), \quad j = 1, \ldots, n, \tag{20b}$$

$$t_e = \sum_{j=1}^{n} s_{ej}, \tag{20c}$$

$$t_e \leq 1, \tag{20d}$$

$$s_{ej} \in \{0, 1\}, \qquad j = 1, \ldots, n. \tag{20e}$$

Proof. We begin with the "only if" part, i.e., suppose that (19) holds. If $x_e > 0$, there exists j_1 such that $x_e = y_{j_1}$. Let $t_e = 1$, $s_{ej_1} = 1$, and $s_{ej} = 0$ $(\forall j \neq j_1)$ to see that (20) is satisfied. Alternatively, if $x_e = 0$, then $t_e = 0$ and $s_{e1} = \cdots = s_{en} = 0$ satisfy (20).

Conversely, suppose that (20) is satisfied. Observe that (20c), (20d), and (20e) imply $t_e \in \{0, 1\}$. If $t_e = 0$, then (20a) implies $x_e = 0$. Moreover, (20c) and (20e) imply $s_{e1} = \cdots = s_{en} = 0$. Therefore, (20b) is reduced to $|y_j| \leq x^{\max}$, which is a redundant constraint. Alternatively, if $t_e = 1$, then (20c) and (20e) imply that there exists j_2 such that $s_{ej_2} = 1$ and $s_{ej} = 0$ for all $j \neq j_2$. Then (20b) is reduced to

$$|x_e - y_{j_2}| \leq 0, \tag{21}$$

$$|x_e - y_j| \leq x^{\max}, \quad \forall j \neq j_2. \tag{22}$$

Here, (21) is equivalent to $x_e = y_{j_2}$, which satisfies (22). Moreover, (20a) is reduced to $0 \leq x_e \leq x^{\max}$, which is a redundant constraint. Thus (19) is satisfied. □

In (20) of Proposition 3.4, we can assume that $y_1, \ldots, y_n$ satisfy

$$x^{\max} \geq y_1 \geq \cdots \geq y_n \geq 0$$

without loss of generality. Accordingly, we see that the design optimization problem can be formulated by adding the following constraints to problem (7):

$$0 \leq x_e \leq x^{\max} t_e, \qquad e = 1, \ldots, m, \tag{23a}$$

$$x^{\max} \geq y_1 \geq \cdots \geq y_n \geq 0, \tag{23b}$$

$$|x_e - y_j| \leq x^{\max}(1 - s_{ej}), \quad e = 1, \ldots, m;\ j = 1, \ldots, n, \tag{23c}$$

$$t_e = \sum_{j=1}^{n} s_{ej}, \qquad e = 1, \ldots, m, \tag{23d}$$

$$t_e \leq 1, \qquad e = 1, \ldots, m, \tag{23e}$$

$$s_{ej} \in \{0, 1\}, \qquad e = 1, \ldots, m;\ j = 1, \ldots, n. \tag{23f}$$

In (23), all the constraints other than (23f) are linear constraints. As a result, we obtain an MISOCP problem, where the continuous variables are x_e, w_e, q_e $(e = 1, \ldots, m)$, and $y_1, \ldots, y_n$ and binary variables are t_e and $s_{e1}, \ldots, s_{en}$ $(e = 1, \ldots, m)$.

Remark 3.5. Problem (7) serves as a continuous relaxation of the MISOCP problem formulated above. To see this, we show that for any $x_e \in [0, x^{\max}]$ $(e = 1, \ldots, m)$ there exist t_e, $s_{ej} \in [0, 1]$ and y_j $(e = 1, \ldots, m; j = 1, \ldots, n)$ satisfying (23a)–(23e). For instance, let $t_e = s_{e1} = x_e / x^{\max}$, $s_{e2} = \cdots = s_{en} = 0$ $(e = 1, \ldots, m)$, and $y_1 = \cdots = y_n = x^{\max}$ to see that these constraints are satisfied. ■

Remark 3.6. In (23), constraints (23d), (23e), and (23f) imply that t_e can become either 0 or 1. Therefore, we can replace (23e) by

$$t_e \in \{0, 1\}, \quad e = 1, \ldots, m$$

without changing the feasible set. In the numerical experiments presented in section 5, $t_1, \ldots, t_m$ are treated as 0-1 variables. ■

Remark 3.7. Variable t_e in (23) serves as a indicator of presence of member e. By using this variable, various constraints on truss topology can be handled within the framework of MISOCP. Two examples are forbiddance of the presence of mutually crossing members and restriction of the number of members connected to a node. These constraints were studied also in, e.g., [13, 27, 34] within the framework of mixed-integer programming. Suppose that members e and e' cross each other in the ground structure. Since $t_e = 1$ if and only if member e exists, forbiddance of crossing means that that t_e and $t_{e'}$ cannot become one simultaneously. This condition can be written as

$$t_e + t_{e'} \leq 1. \tag{24}$$

This constraint is considered in the numerical examples presented in section 5.3. Concerning the degree of a node, i.e., the number of existing members connected to a node, the upper and lower bound constraints are formulated as follows. Let $\rho^{\max}$ denote the specified upper bound. For node

v, we use $\mathcal{E}(v)$ to denote the set of members, in the ground structure, that are connected to node v. Then the upper bound constraint can be written as

$$\sum_{e\in\mathcal{E}(v)} t_e \le \rho^{\max}.$$

The lower bound constraint requires to use an additional 0-1 variable that indicates whether node v exists or vanishes; see [13, 34] for details. ■

Remark 3.8. Condition (20) in Proposition 3.4 (and constraint (23) also) allows $y_j = 0$ and/or $y_j = y_{j'}$ become feasible. It can be also the case that none of $x_1, \ldots, x_m$ take the value of $y_j > 0$. In such cases, the number of different cross-sectional areas used in the corresponding truss design is less than n. Consider an example with $m = 3$ and $n = 2$. We begin with the case in which the number of different cross-sectional areas is exactly $n = 2$. Suppose the member cross-sectional areas are

$$x_1 = 10, \quad x_2 = 6, \quad x_3 = 6.$$

Then y_j and s_{ej} satisfying (20) are determined uniquely as

$$\begin{aligned} &y_1 = 10, \quad s_{11} = 1, \quad s_{21} = 0, \quad s_{31} = 0,\\ &y_2 = 6, \quad\ \ s_{12} = 0, \quad s_{22} = 1, \quad s_{32} = 1. \end{aligned}$$

Next, suppose that the member cross-sectional areas are

$$x_1 = 10, \quad x_2 = 10, \quad x_3 = 0,$$

i.e., the number of different cross-sectional areas is one ($< n$). We can see that there exist y_j and s_{ej} satisfying (23). Such y_j and s_{ej} are not determined uniquely. First, when $y_1 = y_2$, we see that

$$\begin{bmatrix} y_1 \\ y_2 \end{bmatrix} = \begin{bmatrix} 10 \\ 10 \end{bmatrix}, \quad \begin{bmatrix} s_{11} \\ s_{12} \end{bmatrix} \in \left\{ \begin{bmatrix} 1 \\ 0 \end{bmatrix}, \begin{bmatrix} 0 \\ 1 \end{bmatrix} \right\}, \quad \begin{bmatrix} s_{21} \\ s_{22} \end{bmatrix} \in \left\{ \begin{bmatrix} 1 \\ 0 \end{bmatrix}, \begin{bmatrix} 0 \\ 1 \end{bmatrix} \right\}, \quad \begin{bmatrix} s_{31} \\ s_{32} \end{bmatrix} = \begin{bmatrix} 0 \\ 0 \end{bmatrix}$$

satisfy (23). Here, there is no distinguish between adopting y_1 and adopting y_2 for members $e = 1$ and 2. Second, when $0 < y_2 < y_1$, (23) is satisfied with

$$y_1 = 10, \quad y_2 \in]0, 10[, \quad \begin{bmatrix} s_{11} \\ s_{12} \end{bmatrix} = \begin{bmatrix} 1 \\ 0 \end{bmatrix}, \quad \begin{bmatrix} s_{21} \\ s_{22} \end{bmatrix} = \begin{bmatrix} 1 \\ 0 \end{bmatrix}, \quad \begin{bmatrix} s_{31} \\ s_{32} \end{bmatrix} = \begin{bmatrix} 0 \\ 0 \end{bmatrix}.$$

In this case, y_2 is not used for any members. Finally, when $y_2 = 0$, we see that

$$\begin{bmatrix} y_1 \\ y_2 \end{bmatrix} = \begin{bmatrix} 10 \\ 0 \end{bmatrix}, \quad \begin{bmatrix} s_{11} \\ s_{12} \end{bmatrix} = \begin{bmatrix} 1 \\ 0 \end{bmatrix}, \quad \begin{bmatrix} s_{21} \\ s_{22} \end{bmatrix} = \begin{bmatrix} 1 \\ 0 \end{bmatrix}, \quad \begin{bmatrix} s_{31} \\ s_{32} \end{bmatrix} \in \left\{ \begin{bmatrix} 0 \\ 1 \end{bmatrix}, \begin{bmatrix} 0 \\ 0 \end{bmatrix} \right\}$$

also satisfy (23). Here, $s_{32} = 1$ means that $y_2 = 0$ is used for member 3. ■

3.3 Scale-free property

This section establishes a scale-free property of optimal solutions of the problems proposed in section 3.1 and section 3.2.

The optimization problem studied in section 3.1 is obtained by adding the constraint

$$x_e \in \{0, y\}, \quad e = 1, \ldots, m \tag{25}$$

to the conventional compliance minimization problem, (6). Due to this constraint, any feasible solution has uniform cross-sectional areas. On the other hand, a truss design with uniform cross-sectional areas can be obtained by predetermining a cross-sectional area for existing members, like the problems reviewed in section 2.3. This corresponds to solving the conventional problem (6) with adding the constraint

$$x_e \in \{0, \bar{\xi}_1\}, \quad e = 1, \ldots, m, \tag{26}$$

where $\bar{\xi}_1$ is a predetermined positive constant. However, imposing constraint (25) is essentially different from imposing (26). That is, the optimal solution under constraint (25) has a scale-free property as shown below, while this is not the case for the optimal solution under (26).

We recall the scale-free property of the conventional compliance minimization problem, (6). Let $\boldsymbol{x}^*$ denote the optimal solution of problem (6). Assume that the upper bound constraints for the cross-sectional areas,

$$x_e \leq x^{\max}, \quad e = 1, \ldots, m,$$

are inactive at $\boldsymbol{x}^*$. Let α be a constant satisfying

$$\alpha \in]0, x^{\max} / \max\{x_1^*, \ldots, x_m^*\}]. \tag{27}$$

It is worth noting that (27) implies $\alpha x_e^* \leq x^{\max}$ $(e = 1, \ldots, m)$. From the linearity of the stiffness matrix on $\boldsymbol{x}$, (4), and the definition of the compliance, (5), we obtain

$$\pi(\alpha \boldsymbol{x}^*) = \frac{1}{\alpha} \pi(\boldsymbol{x}^*). \tag{28}$$

Suppose that $\bar{V}$ in problem (6) is replaced by $\alpha \bar{V}$. Then we see that $\alpha \boldsymbol{x}^*$ is optimal for the problem after this scaling. Alternatively, if $l_1, \ldots, l_m$ are replaced by $\alpha l_1, \ldots, \alpha l_m$, then $\boldsymbol{x}^*/\alpha$ becomes optimal. Therefore, the optimal solution needs only to be computed for one value of $\bar{V}$ and one geometric scale. The optimal solution corresponding to different values of these quantities can be obtained by applying the scaling explained above. This scale-free property of the conventional compliance optimization of trusses is well known; see, e.g., [8].

In contrast, the optimization problem with constraint (26) does not posses such a scale-free property. This is because, if $\boldsymbol{x}^*$ satisfies (26), $\alpha \boldsymbol{x}^*$ with $\alpha \neq 1$ does not satisfy (26). Similarly, even if we predetermine multiple candidates as

$$x_e \in \{0, \bar{\xi}_1, \ldots, \bar{\xi}_p\}, \quad e = 1, \ldots, m, \tag{29}$$

$\alpha \boldsymbol{x}^*$ does not satisfy (29) in general and the problem lacks the scale-free property. For this reason, when we impose constraint (26) or (29), the optimal truss topology depends on the values of $\bar{V}$ and

$\bar{\xi}_1, \ldots, \bar{\xi}_p$. Concrete examples of this dependence appear in the numerical experiments presented in section 5.1.

The scale-free property of the optimization problem with constraint (25) can be shown as follows. Let $(\boldsymbol{x}^*, y^*)$ be an optimal solution. Then the volume constraint is active at $\boldsymbol{x}^*$. Indeed, if it is inactive, i.e., if

$$\sum_{e=1}^{m} l_e x_e^* < \bar{V}$$

holds, then we see that $(\check{\boldsymbol{x}}, \check{y})$ defined by

$$\check{\boldsymbol{x}} = \frac{\bar{V}}{\sum_{e=1}^{m} l_e x_e^*} \boldsymbol{x}^*, \quad \check{y} = \frac{\bar{V}}{\sum_{e=1}^{m} l_e x_e^*} y^* \tag{30}$$

is feasible for the same problem and that (28) yields

$$\pi(\check{\boldsymbol{x}}) = \frac{\sum_{e=1}^{m} l_e x_e^*}{\bar{V}} \pi(\boldsymbol{x}^*) < \pi(\boldsymbol{x}^*).$$

Let α be a constant satisfying (27). Consider an optimization problem obtained by replacing $\bar{V}$ with $\alpha\bar{V}$. Then $(\alpha\boldsymbol{x}^*, \alpha y^*)$ is feasible for this problem; the structural volume of $\alpha\boldsymbol{x}^*$ is equal to $\alpha\bar{V}$. Suppose for contradiction that it is not optimal, i.e., that there exists a feasible solution, denoted $(\check{\boldsymbol{x}}, \check{y})$, satisfying

$$\pi(\check{\boldsymbol{x}}) < \pi(\alpha\boldsymbol{x}^*) = \pi(\boldsymbol{x}^*)/\alpha.$$

This implies

$$\pi(\check{\boldsymbol{x}}/\alpha) = \alpha\pi(\check{\boldsymbol{x}}) < \pi(\boldsymbol{x}^*). \tag{31}$$

Since $(\check{\boldsymbol{x}}/\alpha, \check{y}/\alpha)$ is feasible for the original problem with upper bound $\bar{V}$, (31) means that $(\boldsymbol{x}^*, y^*)$ is not optimal for the problem with $\bar{V}$, which completes the proof.

Similar consideration can be made for the case in which $l_1, \ldots, l_m$ are replaced by $\alpha l_1, \ldots, \alpha l_m$. Also, the optimization problem proposed in section 3.2 has the same scale-free property.

4 More constraints associated with standardization

This section explores three practical constraints on the cross-sectional areas that can be considered together with the standardization constraint introduced in section 3. These constraints can be handled within the framework of MISOCP.

4.1 Exploring optimal unit amount

Suppose, for simplicity, that a truss consists of members with only three different cross-sectional areas, denoted y_1, y_2, and y_3. Such a truss can actually be obtained as the optimal solution of the MISOCP problem presented in section 3. From a practical point of view, however, not only the number of different cross-sectional ares but also the values of y_j could probably come into an issue. Suppose, for instance, $y_3 \simeq 0$. It is usual that very thin members are not accepted in practice.

Therefore, one may need to round y_3 toward zero and explore a truss design with only two different cross-sectional areas. Alternatively, a practically acceptable lower bound would be given for y_3 and a truss design with three different cross-sectional areas could be explored. On the other hand, suppose that y_3 is practically large but $y_1 \simeq y_2$. In this case, one might be able to explore a truss design with two different cross-sections, probably an intermediate value of y_1 and y_2 and a value close to y_3. In short, when we use some different cross-sectional areas, it might be desired that the values of used cross-sectional areas are distributed almost evenly. This section investigates such a constraint.

As a remedy, we may determine the member cross-sectional areas such that there exists υ (> 0) satisfying

$$x_e \in \{0, \upsilon, 2\upsilon, 3\upsilon\}, \quad \forall e = 1, \ldots, m.$$

Then the cross-sectional areas used in the obtained truss design are, in a sense, equally distributed. It should be clear that υ is considered a design variable. Therefore, the optimization problem retains the scale-free property discussed in section 3.3.

In general, letting n denote the upper bound for the number of different cross-sectional areas, we consider the following constraints:

$$x_e \in \{0, \upsilon, 2\upsilon, \ldots, n\upsilon\}, \quad \forall e = 1, \ldots, m. \tag{32}$$

Here, υ can be interpreted as a unit value of cross-sectional area. In the optimization problem, we explore the optimal unit value as well as the amount of area used for each member. It is worth noting that all of $\upsilon, 2\upsilon, \ldots, n\upsilon$ are not necessarily used in the optimal design.

Constraint (32) can be treated with the formulation proposed in section 3.2. Namely, constraint (32) is satisfied if, in (23), $y_1, \ldots, y_{n-1}$ are multiples of y_n. Thus the optimization problem under consideration can be formulated by adding the linear equality constraints,

$$y_1/n = y_2/(n-1) = \cdots = y_{n-1}/2 = y_n,$$

to the MISOCP problem formulated in section 3.2.

4.2 Selection from predetermined finitely many candidates

In this section we suppose that the cross-sectional area should be chosen from a set of finitely many predetermined candidates. Due to manufacturing and commercial convenience, it is actually often in practice that a member cross-section is chosen among available candidates.

Let $\bar{\xi}_i > 0$ ($i = 1, \ldots, p$) denote the predetermined cross-sectional areas, where p is the number of the available candidates. Then the member cross-sectional area is determined as

$$x_e \in \{0, \bar{\xi}_1, \ldots, \bar{\xi}_p\}. \tag{33}$$

This constraint can be handled by making use of the concept of multiple-choice constraints in integer programming. In the following we combine this constraint with the upper bound constraint for the number of actually adopted candidates.

In the same manner as [29, 34], we use 0-1 variables, $\tau_{e1}, \ldots, \tau_{ep}$, to represent the cross-sectional area used for member e. Let $\tau_{ei} = 1$ if $x_e = \bar{\xi}_i$, otherwise $\tau_{ei} = 0$. Then constraint (33) can be rewritten as

$$x_e = \sum_{i=1}^{p} \bar{\xi}_i \tau_{ei}, \tag{34}$$

$$\sum_{i=1}^{p} \tau_{ei} \leq 1, \tag{35}$$

$$\tau_{ei} \in \{0, 1\}, \quad i = 1, \ldots, p. \tag{36}$$

Note that $x_e = 0$ if and only if $\tau_{e1} = \cdots = \tau_{ep} = 0$.

The constraint on the variation of cross-sectional areas can be formulated as follows. First, suppose that the truss should consist of members with uniform cross-sectional areas. This means that there exists $y \in \mathbb{R}$ such that $x_1, \ldots, x_m$ satisfy $x_e \in \{0, y\}$ and (33). Like section 3.1, we use variable t_e such that $t_e = 1$ means $x_e > 0$ and $t_e = 0$ means $x_e = 0$. From (34), (35), and (36), t_e can be represented in terms of $\tau_{e1}, \ldots, \tau_{ep}$ as

$$t_e = \sum_{i=1}^{p} \tau_{ei}. \tag{37}$$

It follows from Proposition 3.1 that the uniformity constraint is satisfied if and only if all the members satisfy

$$|x_e - y| \leq x^{\max}(1 - t_e), \tag{38}$$

where $x^{\max} = \max\{\bar{\xi}_1, \ldots, \bar{\xi}_p\}$. The upshot is that the optimization problem under consideration can be formulated as an MISOCP by adding constraints (34), (35), (36), (37), and (38) to problem (7).

We next consider the case in which at most n different candidates are allowed to be used as member cross-sectional areas. In the same manner as Proposition 3.4, we use continuous variables $y_1, \ldots, y_n$ to denote the cross-sectional areas that are actually used in a truss design. For member e, the selected cross-sectional area is represented by using 0-1 variables $s_{e1}, \ldots, s_{en}$ so that $s_{ej} = 1$ means $x_e = y_j$. This condition can be rewritten as

$$|x_e - y_j| \leq x^{\max}(1 - s_{ej}), \quad j = 1, \ldots, n. \tag{39}$$

It should be clear that x_e is subjected to constraints (34), (35), and (36), which is equivalent to (33). Hence, $s_{ej} = 1$ in (39) implies $y_j \in \{0, \bar{\xi}_1, \ldots, \bar{\xi}_p\}$, although y_j is treated as a continuous variable. For member e, exactly one of $s_{e1}, \ldots, s_{en}$ should become 1 if $x_e > 0$, while $s_{e1} = \cdots = s_{en} = 0$ if $x_e = 0$. This condition can be formulated by using $\tau_{e1}, \ldots, \tau_{ep}$ as

$$\sum_{j=1}^{n} s_{ej} = \sum_{i=1}^{p} \tau_{ei}. \tag{40}$$

Consequently, the design optimization problem under consideration can be formulated as an MISOCP problem by adding constraints (34), (35), (36), (39), (40), and

$$s_{ej} \in \{0, 1\}, \quad j = 1, \ldots, n \tag{41}$$

to problem (7).

Remark 4.1. Like the formulations presented in section 3, the continuous relaxations of the MISOCP problems formulated in section 4 are SOCP problem (7), and hence the continuous compliance optimization problem in (6). This correspondence might be a particular attribute of the MISOCP formulations presented in this paper. For comparison, we may consider an alternative formulation of the problem studied in this section. Indeed, when the set of candidate cross-sectional areas is given, it is possible to recast the optimization problem as an MILP problem, by adding constraints (39), (40), and (41) to MILP problem (9). The obtained MILP problem then involves M, a sufficiently large constant. For this reason, the continuous relaxation of this MILP problem is in general different from the continuous compliance optimization problem in (6); the feasible set of problem (6) is a subset of that of the MILP problem. Thus the proposed MISOCP problem has a tighter continuous relaxation than the MILP formulation. ■

4.3 Selection from predetermined multiples

As a special case of (33) in section 4.2, we next suppose that the cross-sectional area should be chosen among multiples of a predetermined unit value. In this case the number of integer variables can be reduced drastically, which may speed up the solution process.

Suppose that the member cross-sectional area is to be determined as

$$x_e \in \{0, \bar{\delta}, 2\bar{\delta}, \ldots, p\bar{\delta}\}, \tag{42}$$

where $\bar{\delta} > 0$ is a predetermined constant. It is known that (42) can be expressed by using only $\lfloor \log_2 p \rfloor + 1$ binary variables; see, e.g., [10]. Namely, (42) can be rewritten as

$$x_e = \bar{\delta} \sum_{l=1}^{r} 2^{l-1} \tilde{\tau}_{el}, \tag{43}$$

$$\tilde{\tau}_{el} \in \{0, 1\}, \quad l = 1, \ldots, r, \tag{44}$$

$$x_e \leq x^{\max}, \tag{45}$$

where we use $r = \lfloor \log_2 p \rfloor + 1$ and $x^{\max} = p\bar{\delta}$ for notational simplicity.[2]

The binary expansion in (43), (44), and (45) can be combined with the constraint on the number of different cross-sectional areas as follows. We begin with the uniformity constraint. The key idea is again Proposition 3.1. For member e, we use variable t_e such that $t_e = 0$ means $x_e = 0$ and $t_e = 1$ means $x_e > 0$. It follows from (43) and (44) that t_e can be related to $\tilde{\tau}_{e1}, \ldots, \tilde{\tau}_{er}$ as

$$t_e = \begin{cases} 0 & \text{if } \tilde{\tau}_{e1} = \cdots = \tilde{\tau}_{er} = 0, \\ 1 & \text{otherwise.} \end{cases} \tag{46}$$

Since $\tilde{\tau}_{e1}, \ldots, \tilde{\tau}_{er}$ are 0-1 variables, relation (46) can be reduced to the following linear inequality constraints:

$$t_e \leq \sum_{l=1}^{r} \tilde{\tau}_{el}, \tag{47}$$

$$t_e \geq \tilde{\tau}_{el}, \quad l = 1, \ldots, r, \tag{48}$$

$$t_e \leq 1. \tag{49}$$

[2]Constraints (43) and (44) imply $x_e \in \{0, \bar{\delta}, 2\bar{\delta}, \ldots, (2^r - 1)\bar{\delta}\}$.

Then x_e should take the same value for all e such that $t_e = 1$, which can be rewritten as

$$|x_e - y| \leq x^{\max}(1 - t_e). \tag{50}$$

Thus we attain an MISOCP formulation by adding constraints (43), (44), (45), (47), (48), (49), and (50) to problem (7).

Remark 4.2. Constraints (48) and (49) imply $t_e \in \{0, 1\}$, because $\tilde{\tau}_{el} \in \{0, 1\}$ $(l = 1, \ldots, r)$. Therefore, we can replace (49) by $t_e \in \{0, 1\}$. Actually we treat t_e as a binary design variable in the numerical experiments presented in section 5. ■

We next suppose that at most n different cross-sectional areas can be used in a truss design. According to Proposition 3.4, we formulate this condition with variables $y_j \in \mathbb{R}$ and $s_{ej} \in \{0, 1\}$ as (20b). Variables $s_{e1}, \ldots, s_{en}$ are related to variable t_e, which serves as an indicator of existence of member e, through (20c). Moreover, relation between t_e and $\tilde{\tau}_{e1}, \ldots, \tilde{\tau}_{er}$ is given by (47) and (48). The upshot is that we add the following constraints to problem (7):

$$x_e = \sum_{l=1}^{r} 2^{l-1} \tilde{\tau}_{el} \leq x^{\max}, \qquad e = 1, \ldots, m, \tag{51a}$$

$$x^{\max} \geq y_1 \geq \cdots \geq y_n \geq 0, \tag{51b}$$

$$|x_e - y_j| \leq x^{\max}(1 - s_{ej}), \quad e = 1, \ldots, m;\ j = 1, \ldots, n, \tag{51c}$$

$$t_e = \sum_{j=1}^{n} s_{ej} \leq 1, \qquad e = 1, \ldots, m, \tag{51d}$$

$$t_e \leq \sum_{l=1}^{r} \tilde{\tau}_{el}, \qquad e = 1, \ldots, m, \tag{51e}$$

$$t_e \geq \tilde{\tau}_{el}, \qquad e = 1, \ldots, m;\ l = 1, \ldots, r, \tag{51f}$$

$$s_{ej} \in \{0, 1\}, \qquad e = 1, \ldots, m;\ j = 1, \ldots, n, \tag{51g}$$

$$\tilde{\tau}_{el} \in \{0, 1\}, \qquad e = 1, \ldots, m;\ l = 1, \ldots, r. \tag{51h}$$

Here, all the constraints other than (51g) and (51h) are linear constraints. Therefore, the resulting optimization problem is still an MISOCP problem.

Remark 4.3. Since (51d) and (51g) imply $t_e \in \{0, 1\}$, we can treat t_e as a 0-1 variable. This is done in the numerical experiments in section 5. ■

5 Numerical experiments

This section presents numerical experiments on the proposed MISOCP formulations. We examine computational efficiency and study some properties of optimal solutions with standardization constraints on design variables. MISOCP problems were solved by using CPLEX ver. 12.6 [19]. The data of the problems were prepared in the CPLEX LP file format with MATLAB ver. 7.13. Computation was carried out on two 2.66 GHz 6-Core Intel Xeon Westmere processors with 64 GB RAM.

The `mip strategy miqcpstrat` parameter of CPLEX is set to two (solving an LP relaxation of the MISOCP model at each node) and `mip cuts all` parameter is set to one (generating all types

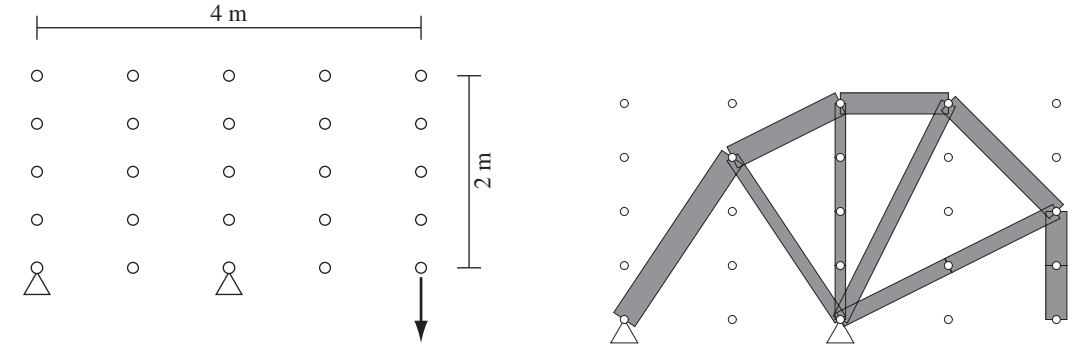

Figure 1: Example (I). (a) The problem setting; and (b) the optimal solution of the continuous optimization problem.

of cuts moderately). These parameters were determined by preliminary numerical experiments. The integrality tolerance in CPLEX is set to 0 and the feasibility tolerance in the simplex method is set to 10^{-8}. The other parameters of CPLEX are set to the default values.

Table 1: Computational results of example (I) in cases A and B. The optimal solutions are shown in Figure 2.

			Areas (mm^2)			
Case	n	Obj. (J)	y_1	y_2	y_3	Time (s)
A-1 ≡ B-1	1	497.38	1095.15	—	—	13.2
A-2	2	469.55	1380.90	736.34	—	16.2
A-3	3	465.63	1403.07	976.98	721.14	33.5
B-2	2	469.94	1404.52	702.26	—	22.7
B-3	3	469.07	1035.71	690.47	345.24	44.3

Table 2: Computational results of example (I) in case C. The optimal solutions are shown in Figure 3.

Case	Cand. areas (mm^2)	Obj. (J)	Vol. (mm^3)	Time (s)
C1	$\{0, 1000\}$	525.69	15.795×10^6	8.0
C2	$\{0, 1050\}$	518.77	15.340×10^6	6.8
C3	$\{0, 1100\}$	515.20	15.756×10^6	18.5
C4	$\{0, 700, 1400\}$	471.45	15.949×10^6	12.9
C5	$\{0, 400, 800, 1200\}$	475.14	15.982×10^6	18.3
C6	$\{0, 600, 1200, 1800\}$	475.04	15.941×10^6	9.6

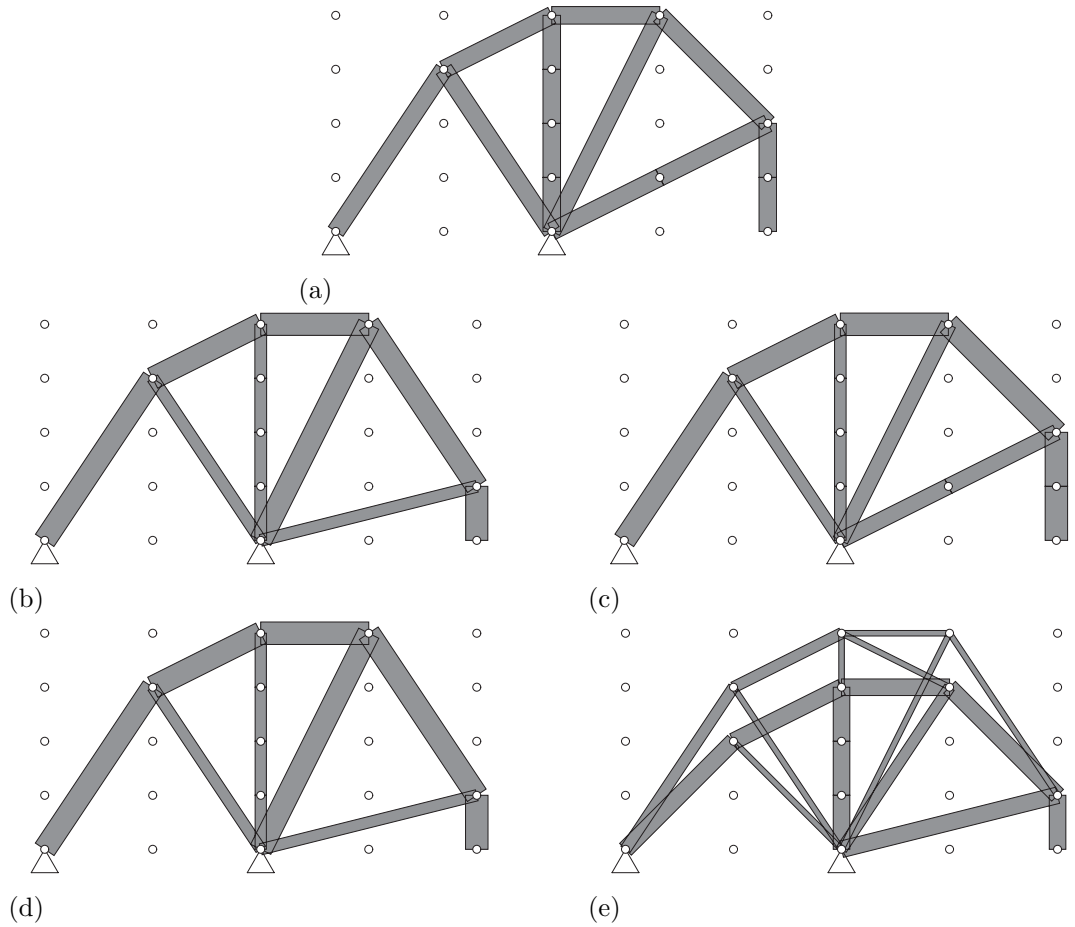

Figure 2: The optimal solutions of example (I) in cases A and B. The solutions in (a) cases A and B with $n = 1$ (i.e., A-1 and B-1); (b) case A with $n = 2$ (A-2); (c) case A with $n = 3$ (A-3); (d) case B with $n = 2$ (B-2); and (e) case B with $n = 3$ (B-3).

5.1 Example (I)

Consider the design domain shown in Figure 1(a), where only the nodes of a ground structure are depicted. Any two nodes are connected by a member, but overlapping of members is avoided by removing the longer member when two members overlap. The ground structure has $m = 200$ members and $d = 46$ degrees of freedom of displacements. The leftmost and middle nodes in the bottom row are pin-supported. A vertical force of 100 kN is applied at the bottom rightmost node. The specified upper bound for the structural volume is $\bar{V} = 16 \times 10^6\,\mathrm{mm}^3$. The upper bound for the member cross-sectional areas is $x^{\max} = 2000\,\mathrm{mm}^2$. The elastic modulus is 200 GPa. Similar examples have been solved in [1, 34].

The optimal solution of the conventional compliance minimization problem, i.e., the continuous relaxation problem, is shown in Figure 1(b), where the width of each member is proportional to its cross-sectional area. The optimal value is 462.59 J. The maximum cross-sectional area in this solution is $1580.53\,\mathrm{mm}^2$. Since members aligned in a straight line have the same cross-sectional areas, this solution has 9 different member cross-sectional areas.

As for standardization constraints, we consider four cases:

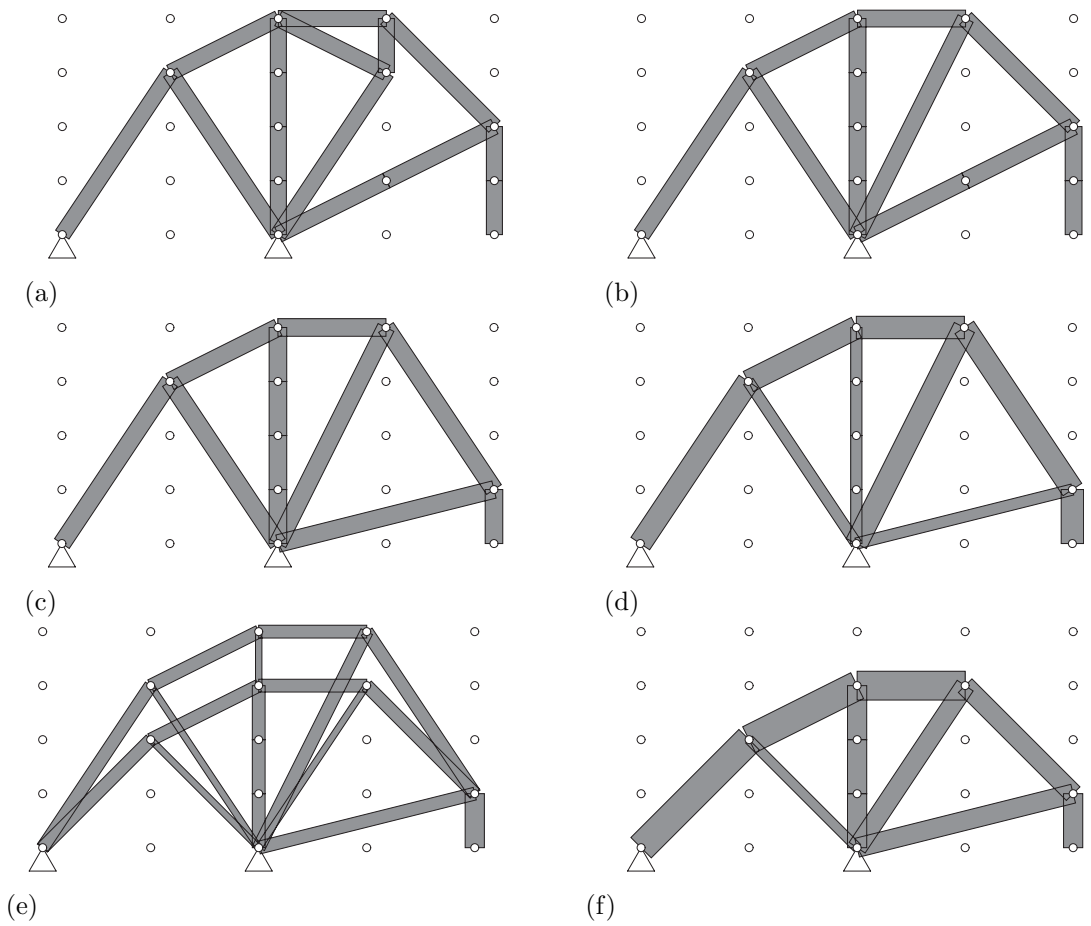

Figure 3: The optimal solutions of example (I) in case C. The solutions in (a) case C1; (b) case C2; (c) case C3; (d) case C4; (e) case C5; and (f) case C6.

- Case A: The adopted values of cross-sectional areas are explored freely. The optimization problems formulated in sections 3.1 and 3.2 are solved.
- Case B: The adopted values of cross-sectional areas forms a set of multiples of a unit value, which is also a design variable. The optimization problem formulated in section 4.1 is solved.
- Case C: The cross-sectional areas are selected among a few of predetermined candidates. The optimization problem formulated in section 4.3 without the constraint on the number of different cross-sectional areas is solved.
- Case D: The cross-sectional areas are selected among a large number of predetermined candidates. The optimization problem formulated in section 4.3 with the constraint on the number of different cross-sectional areas is solved.

Note that the volume constraint becomes active at the optimal solutions in cases A and B.

With $n = 1$, i.e., with the uniformity constraint on the cross-sectional areas, the optimal solutions in cases A and B certainly coincide. This optimal solution is shown in Figure 2(a). The member cross-sectional areas and the compliance, together with the computational time required by CPLEX, are reported in Table 1. It is worth noting that, as seen in Figures 1(b) and 2(a), the optimal solution

with uniform cross-sectional areas has the same topology as the optimal solution of the continuous relaxation problem. The increase of the objective value is about 7.5%. Thus, at the expense of small increase of compliance, we can enjoy the advantage of member standardization.

The optimal solutions in case A with $n = 2$ (called case A-2) and $n = 3$ (called case A-3) are shown in Figure 2(b) and Figure 2(c), respectively. The computational results are listed in Table 1. As expected, the optimal value decreases as n increases. The set of members used in case A-2 (shown in Figure 2(b)) is different from the one in the continuous relaxation solution (in Figure 1(b)). In contrast, the solution in case A-3 (in Figure 2(c)) has the same members as the continuous relaxation solution.

Figures 2(d) and 2(e) show the optimal solutions in case B with $n = 2$ (called case B-2) and $n = 3$ (called case B-3). The solution in case B-2 has the same structural topology as that in case A-2. In contrast, the solution in case B-3 is much different from the other solutions. This solution has two arches that are connected to each other by a thin member. In case A-1, the MISOCP problem has $m = 200$ binary variables. In cases A-3 and B-3, we use $nm = 600$ variables for s_{ej} and $m = 200$ variables for t_e (the latter is optional as mentioned in Remark 3.6).

In case C, we assume that the number of predetermined candidate areas is relatively small. Hence, the upper bound constraint for the number of different cross-sectional areas is not considered. For comparison with cases A and B, we consider six problems:

- Case C1: $x_e \in \{0, 1000\}$ in mm^2.
- Case C2: $x_e \in \{0, 1050\}$ in mm^2.
- Case C3: $x_e \in \{0, 1100\}$ in mm^2.
- Case C4: $x_e \in \{0, 700, 1400\}$ in mm^2.
- Case C5: $x_e \in \{0, 600, 1200, 1800\}$ in mm^2.
- Case C6: $x_e \in \{0, 400, 800, 1200\}$ in mm^2.

We use $r = 2$ in (43) for cases C4, C5, and C6, while $r = 1$ for cases C1, C2, and C3. The optimal solutions are collected in Figure 3. Problems with single candidate area are examined in cases C1, C2, and C3. The candidate values of these problems are determined to be close to the optimal solution in case A-1, i.e., $1095.15\,\mathrm{mm}^2$. The optimal solutions in cases C1 and C3 (shown in Figure 3(a) and Figure 3(c), respectively) include some members different from the members exist in the optimal solution in case A-1 (in Figure 2(a)). In contrast, the optimal solution in case C2 (shown in Figure 3(b)) has the same topology as case A-1. However, the optimal value in case C2 is larger than that in case A-1, because the volume constraint is inactive in case C2. Thus the optimal topology with uniform cross-sectional areas highly depends on the predetermined value of cross-sectional areas. Therefore, it may not be easy to guess the predetermined value such that the optimal solution has the same topology as the solution in case A-1, which has a scale-free property. The optimal solution in case C4 (shown in Figure 3(d)) is very similar to those in cases A-2 and B-2 (in Figure 2(b) and Figure 2(d)). The optimal solution in case C5 has two arches. The optimal solution in case C6 has low rise.

Finally, as case D, we consider a large number of candidate cross-sectional areas and simultaneously impose the constraint on the number of different cross-sectional areas. As for the set of candidate cross-sectional areas, we consider three cases:

- Case D1: $\bar{\delta} = 250\,\mathrm{mm}^2$ and $p = 7$, i.e., $x_e \in \{0, 250, 500, \ldots, 1750\}$ in mm^2.
- Case D2: $\bar{\delta} = 120\,\mathrm{mm}^2$ and $p = 15$, i.e., $x_e \in \{0, 120, 240, \ldots, 1800\}$ in mm^2.
- Case D3: $\bar{\delta} = 125\,\mathrm{mm}^2$ and $p = 15$, i.e., $x_e \in \{0, 125, 250, \ldots, 1875\}$ in mm^2.

Note that we use $r = 3$ in (43) for case D1 and $r = 4$ for cases D2 and D3. As for the upper bound for the number of different cross-sectional areas, we consider three cases: $n = 1$, 2, and 3. Figure 4 collects the optimal solutions. The computational results are listed in Table 3. Here, for example, "D2-3" denotes the problem instance in which we select at most $n = 3$ different cross-sectional areas from the set considered in case D2. The number of members that have cross-sectional area y_j is also reported in this table. For instance, the solution in case D1-2 consists of eight members with cross-sectional area $y_1 = 1500\,\mathrm{mm}^2$ and four members with cross-sectional area $y_2 = 750\,\mathrm{mm}^2$.

For $n = 1$, the solution in case D2-1 has the best compliance. For $n = 2$ and 3, the solutions in cases D3-2 and D3-3 are best. The solution in case D2-2 (shown in Figure 4(e)) essentially consists of two arches (connected to each other by a single thin member). The solutions in cases D1-1 and D3-1 (in Figure 4(a) and Figure 4(g)) are same and have very many members. These solutions and the solution in case D1-2 (in Figure 4(b)) have horizontal members that connect the right support and the load point. The solutions in D1-3 and D2-3 have the same topology. Also, topologies of the solutions in cases D2-1, D3-2, and D3-3 are same. Thus the optimal solution highly depends on the set of candidate cross-sectional areas. It is observed in Table 3 that the computational cost increases as n increases. The largest computational time is required in case D2-3 and is about 19 minutes. The number of 0-1 variables in cases D2-3 and D3-3 is $8m = 1600$.

Table 3: Computational results of example (I) in case D. The optimal solutions are shown in Figure 4.

				Areas (mm^2)			
Case	n	Obj. (J)	Vol. (mm^3)	y_1	y_2	y_3	Time (s)
D1-1	1	508.95	15.983×10^6	(25@) 500	—	—	25.2
D1-2	2	479.50	15.967×10^6	(8@) 1500	(4@) 750	—	90.9
D1-3	3	469.70	15.999×10^6	(3@) 1500	(3@) 1250	(6@) 750	220.3
D2-1	1	504.36	15.779×10^6	(14@) 1080	—	—	22.8
D2-2	2	477.47	15.934×10^6	(12@) 840	(10@) 360	—	139.3
D2-3	3	469.57	15.956×10^6	(3@) 1440	(3@) 1320	(6@) 720	1,113.2
D3-1	1	508.95	15.983×10^6	(25@) 500	—	—	34.7
D3-2	2	471.69	15.951×10^6	(6@) 1375	(8@) 875	—	68.3
D3-3	3	469.35	15.990×10^6	(3@) 1375	(6@) 1125	(5@) 750	502.3

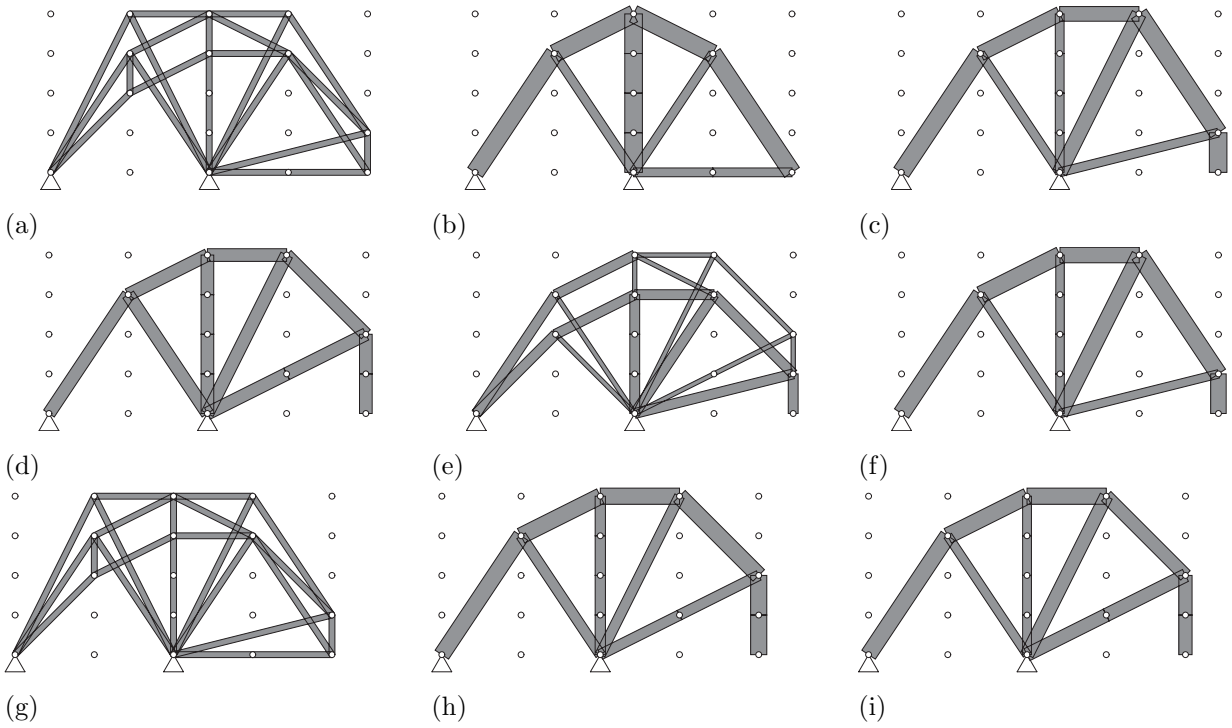

Figure 4: The optimal solutions of example (I) in case D. The solutions in (a) case D1 with $n = 1$ (i.e., D1-1); (b) case D1 with $n = 2$ (D1-2); (c) case D1 with $n = 3$ (D1-3); (d) case D2 with $n = 1$ (D2-1); (e) case D2 with $n = 2$ (D2-2); (f) case D2 with $n = 3$ (D2-3); (g) case D3 with $n = 1$ (D3-1); (h) case D3 with $n = 2$ (D3-2); and (i) case D3 with $n = 3$ (D3-3).

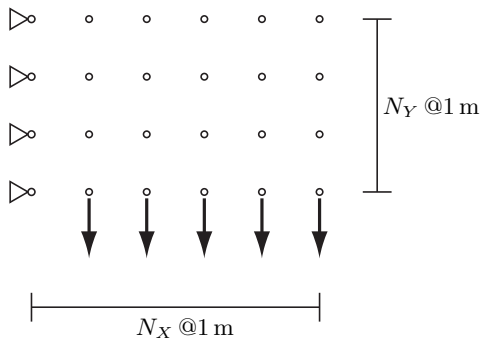

Figure 5: Example (II). The problem setting for $(N_X, N_Y) = (5, 3)$.

5.2 Example (II)

We next consider the design domain shown in Figure 5. Only the nodes of a ground structure are depicted, but any two nodes are connected by a member. Overlapping of members is avoided by removing the longer members. The leftmost nodes of the ground structure are pin-supported. As for the size of the ground structure, we consider two cases, $(N_X, N_Y) = (4, 3)$ and $(5, 3)$. The number of members, m, and the number of degrees of freedom of displacements, d, are listed in Table 4. In this example we consider single and multiple load scenarios. A vertical force of 20 kN is applied at each bottom node. In a single load scenario these external forces are applied to the nodes simultaneously and the compliance corresponding to this scenario is minimized. In a multiple load scenario, in contrast, we suppose that each external force is applied to the corresponding node

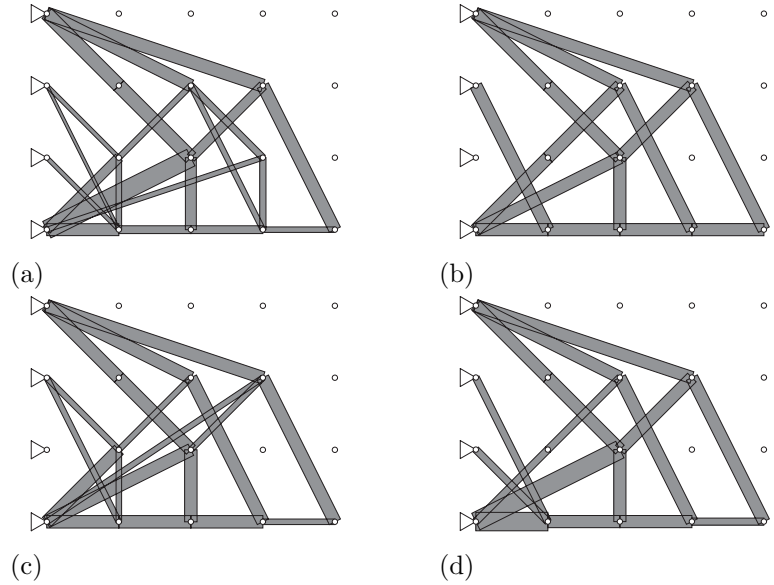

Figure 6: The optimal solutions of example (II) with $(N_X, N_Y) = (4, 3)$ in a single load case. (a) The continuous solution; (b) the solution for $n = 1$; (c) the solution for $n = 2$; and (d) the solution for $n = 3$.

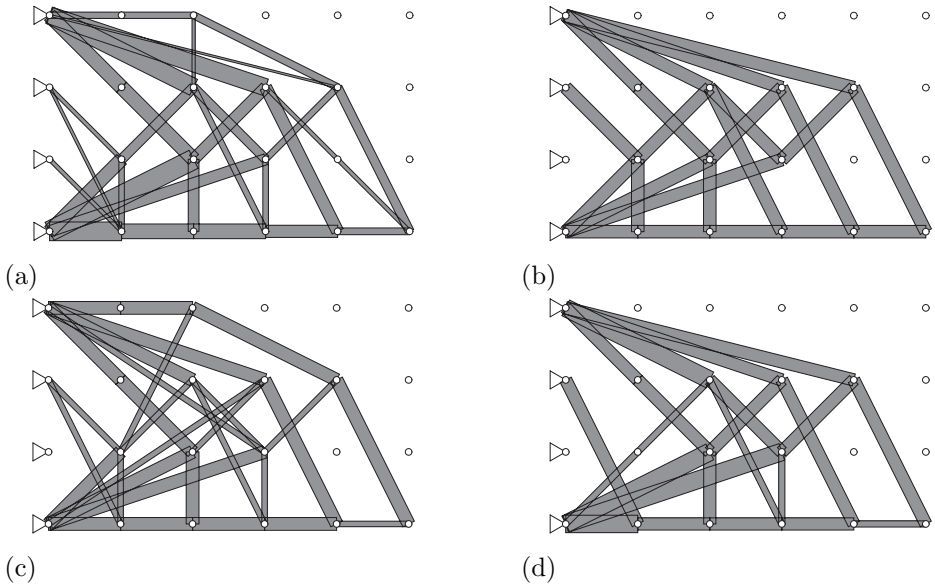

Figure 7: The optimal solutions of example (II) with $(N_X, N_Y) = (5, 3)$ in a single load case. (a) The continuous solution; (b) the solution for $n = 1$; (c) the solution for $n = 2$; and (d) the solution for $n = 3$.

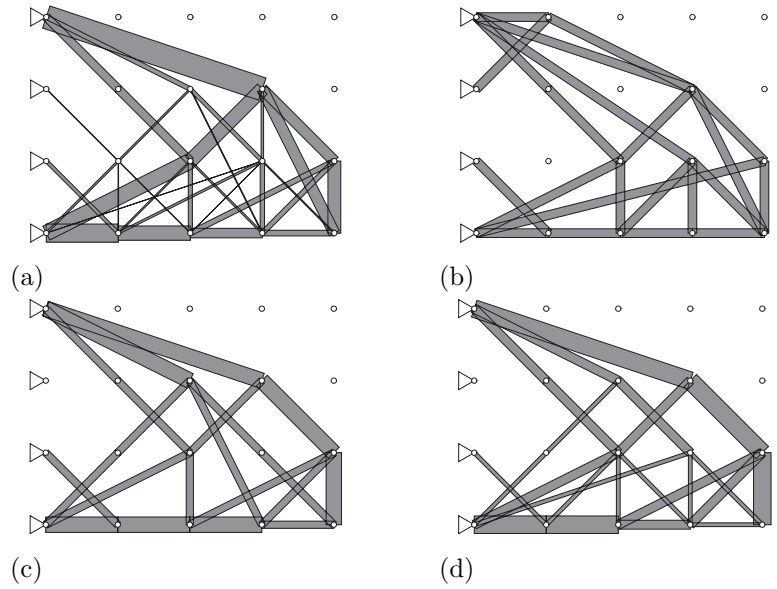

Figure 8: The optimal solutions of example (II) with $(N_X, N_Y) = (4, 3)$ in a multiple load case. (a) The continuous solution; (b) the solution for $n = 1$; (c) the solution for $n = 2$; and (d) the solution for $n = 3$.

separatedly. Hence there exist N_X loading scenarios and the maximum compliance is minimized. The upper bounds for the structural volume are listed in Table 4. The upper bound for the member cross-sectional areas is $x^{\max} = 1000\,\mathrm{mm}^2$. The elastic modulus is 200 GPa. Only the formulations in section 3 are considered.

Figure 6 and Figure 7 collect the optimal solutions with the single loading scenarios. The optimal solutions of the continuous relaxation problem are shown in Figure 6(a) and Figure 7(a). The optimal values of these solutions are reported in the column "cont. opt." of Table 4. Table 5 reports the computational results with the upper bound constraint for the number of different cross-sectional areas. The optimal solution with $(N_X, N_Y) = (4, 3)$ and $n = 1$ is shown in Figure 6(b). The load-bearing mechanism of this solution is essentially similar to that of the continuous solution in Figure 6(a); indeed, the set of existing members of the solution with $n = 1$ is a subset of that of the

Table 4: Characteristics of the problem instances in examples (II) and (III).

Ex.	(N_X, N_Y)	m	d	$\bar{V}$ (mm^3)	Cont. opt. (J)
(II)	$(4, 3)$	131	32	12.0×10^6	142.59
(II)	$(5, 3)$	188	40	15.0×10^6	289.33
(III)	$(6, 2)$	140	36	12.0×10^6	3504.17
(III)	$(7, 2)$	181	42	14.0×10^6	4889.29
(III)	$(6, 4)$	386	60	24.0×10^6	720.75
(III)	$(7, 4)$	503	70	28.0×10^6	969.45
(III)	$(5, 6)$	559	70	30.0×10^6	214.07
(III)	$(6, 6)$	748	84	36.0×10^6	300.71

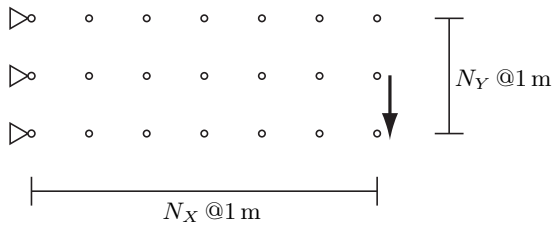

Figure 9: Example (III). The problem setting for $(N_X, N_Y) = (6, 2)$.

continuous solution. The optimal solution with $n = 2$, shown in Figure 6(c), has one member that does not exist in the continuous optimal solution. The optimal solution with $n = 3$ in Figure 6(d) is very close to the continuous one, although the latter has five extra thin members.

In the case of $(N_X, N_Y) = (5, 3)$, the set of nodes used in the optimal solution with $n = 1$ (in Figure 7(b)) is apparently different from that in the continuous solution in Figure 7(a). The topology of the solution with $n = 3$ (in Figure 7(d)) is similar to that of the solution with $n = 1$. The computational time required to solve the problem with $n = 3$ is about half an hour.

Figure 8 collects the optimal solutions in the multiple load scenarios. The optimal value of the continuous solution, shown in Figure 8(a), is 27.564 J. It is observed in Figure 8 that, as n increases, the optimal solution becomes close to the continuous one. Actually the set of existing members in each of Figure 8(c) and Figure 8(d) is a subset of that in Figure 8(a). Since $N_X = 4$ loading conditions are considered, the MISOCP formulation involves $4m = 524$ second-order cone constraints. It is observed from Table 5 that very large computational costs are required compared to the single load problems. Particularly, the computational time required to solve the problem with $n = 3$ is more than 30 hours.

Table 5: Computational results of example (II). The optimal solutions are shown in Figure 6, Figure 7, and Figure 8.

				Areas (mm^2)				
(N_X, N_Y)	n	Load	Obj. (J)	y_1	y_2	y_3	Time (s)	# of nodes
$(4, 3)$	1	single	150.85	454.31	—	—	5.8	2,291
$(4, 3)$	2	single	144.75	466.13	208.09	—	10.6	18,775
$(4, 3)$	3	single	143.61	690.99	455.74	262.73	101.1	126,466
$(5, 3)$	1	single	307.78	375.55	—	—	23.3	14,738
$(5, 3)$	2	single	295.05	383.38	165.85	—	213.2	204,316
$(5, 3)$	3	single	291.38	522.75	366.08	185.53	1,709.8	970,011
$(4, 3)$	1	multiple	32.448	325.09	—	—	4,310.9	93,897
$(4, 3)$	2	multiple	29.141	577.50	268.51	—	83,657.4	614,074
$(4, 3)$	3	multiple	28.380	656.46	334.29	142.40	112,934.3	2,005,090

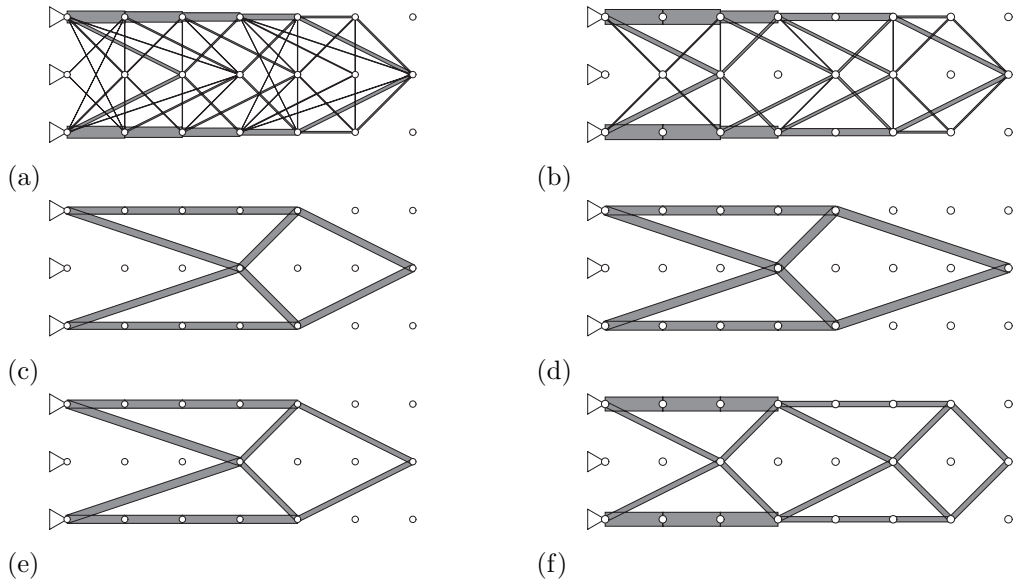

Figure 10: The optimal solutions of example (III) for $(N_X, N_Y) = (6, 2)$ and $(N_X, N_Y) = (7, 2)$. The solutions for (a) $(6, 2)$ without the standardization constraint; (b) $(7, 2)$ without the standardization constraint; (c) $(6, 2)$ with $n = 1$; (d) $(7, 2)$ with $n = 1$; (e) $(6, 2)$ with $n = 2$; and (f) $(7, 2)$ with $n = 2$.

Table 6: Computational results of example (III). The optimal solutions are shown in Figure 10, Figure 11, and Figure 12.

				Areas (mm^2)			
(N_X, N_Y)	n	Cross. const.	Obj. (J)	y_1	y_2	Time (s)	# of nodes
$(6, 2)$	1	off	3677.69	554.91	—	7.3	2,092
$(6, 2)$	2	off	3542.58	632.28	403.10	29.9	31,555
$(7, 2)$	1	off	5453.24	596.31	—	38.5	8,798
$(7, 2)$	2	off	4996.59	935.74	357.90	77.6	31,803
$(6, 4)$	1	off	742.79	967.77	—	202.1	48,222
$(6, 4)$	2	off	723.48	1540.90	438.49	137.7	29,884
$(7, 4)$	1	off	1014.09	1041.11	—	278.2	31,751
$(7, 4)$	2	off	987.22	934.24	328.66	1,015.8	97,708
$(7, 4)$	2	on	988.40	1116.07	665.28	700.8	30,662
$(5, 6)$	1	off	231.12	846.63	—	2,778.5	281,388
$(5, 6)$	1	on	240.52	1261.95	—	4,177.6	115,551
$(6, 6)$	1	off	323.20	885.02	—	24,850.6	849,940
$(6, 6)$	1	on	328.74	1320.58	—	25,679.9	379,267

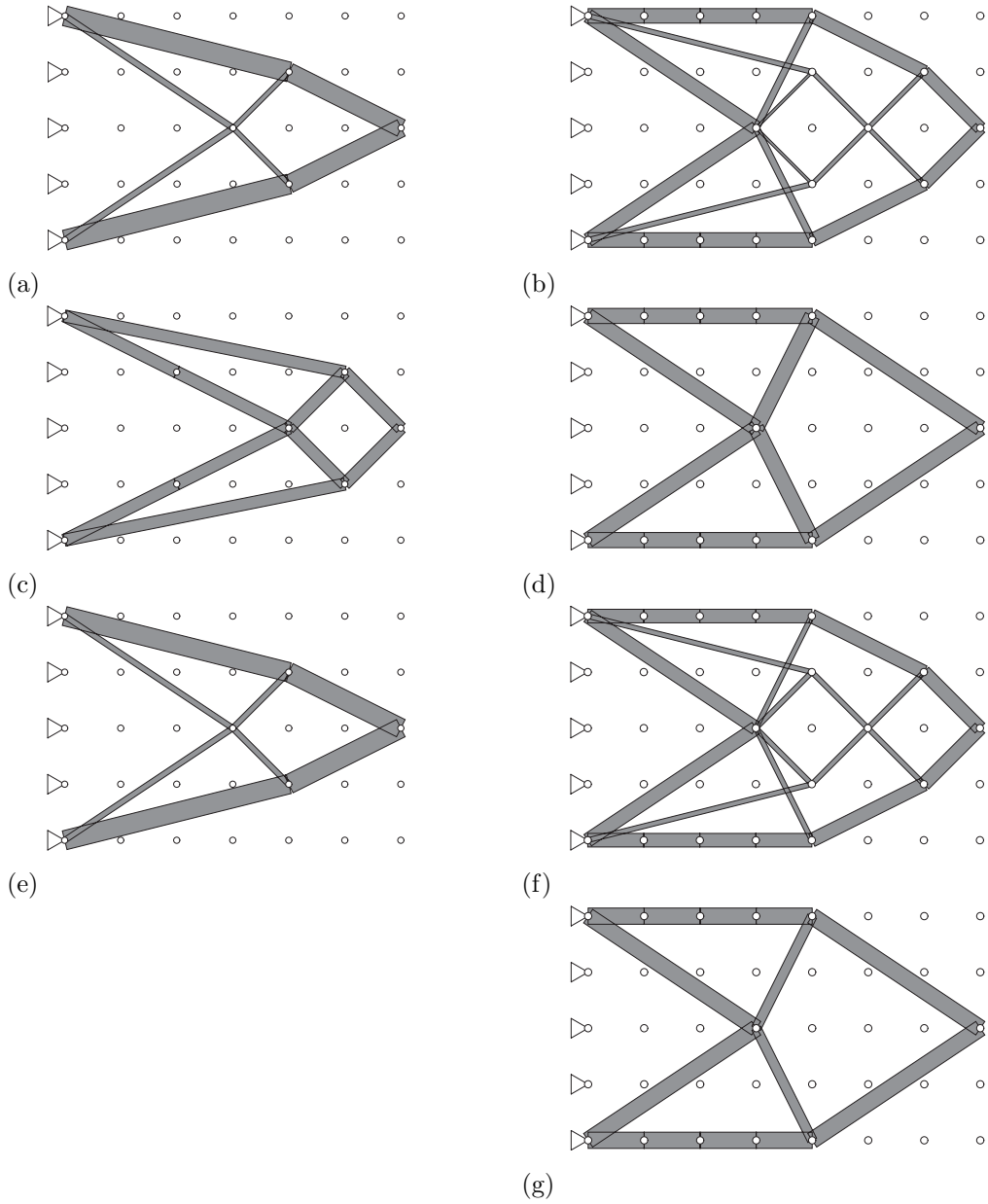

Figure 11: The optimal solutions of example (III) for $(N_X, N_Y) = (6, 4)$ and $(N_X, N_Y) = (7, 4)$. The solutions for (a) $(6, 4)$ without the standardization constraint; (b) $(7, 4)$ without the standardization constraint; (c) $(6, 4)$ with $n = 1$; (d) $(7, 4)$ with $n = 1$; (e) $(6, 4)$ with $n = 2$; (f) $(7, 4)$ with $n = 2$; and (g) $(7, 4)$ with $n = 2$ and the constraints prohibiting presence of mutually crossing members.

5.3 Example (III)

Consider the cantilever problem in Figure 9. In this example we consider the constraint prohibiting the presence of mutually crossing members when the optimal solution without this constraint has mutually crossing members. As for problem size, we consider six cases, $(N_X, N_Y) = (6, 2)$, $(7, 2)$, $(6, 4)$, $(7, 4)$, $(5, 6)$, and $(6, 6)$. Table 4 lists the number of members, the number of degrees of freedom of displacements, the upper bound for the structural volume, and the optimal value of the continuous relaxation problem. A vertical force of 100 kN is applied at the rightmost middle node.

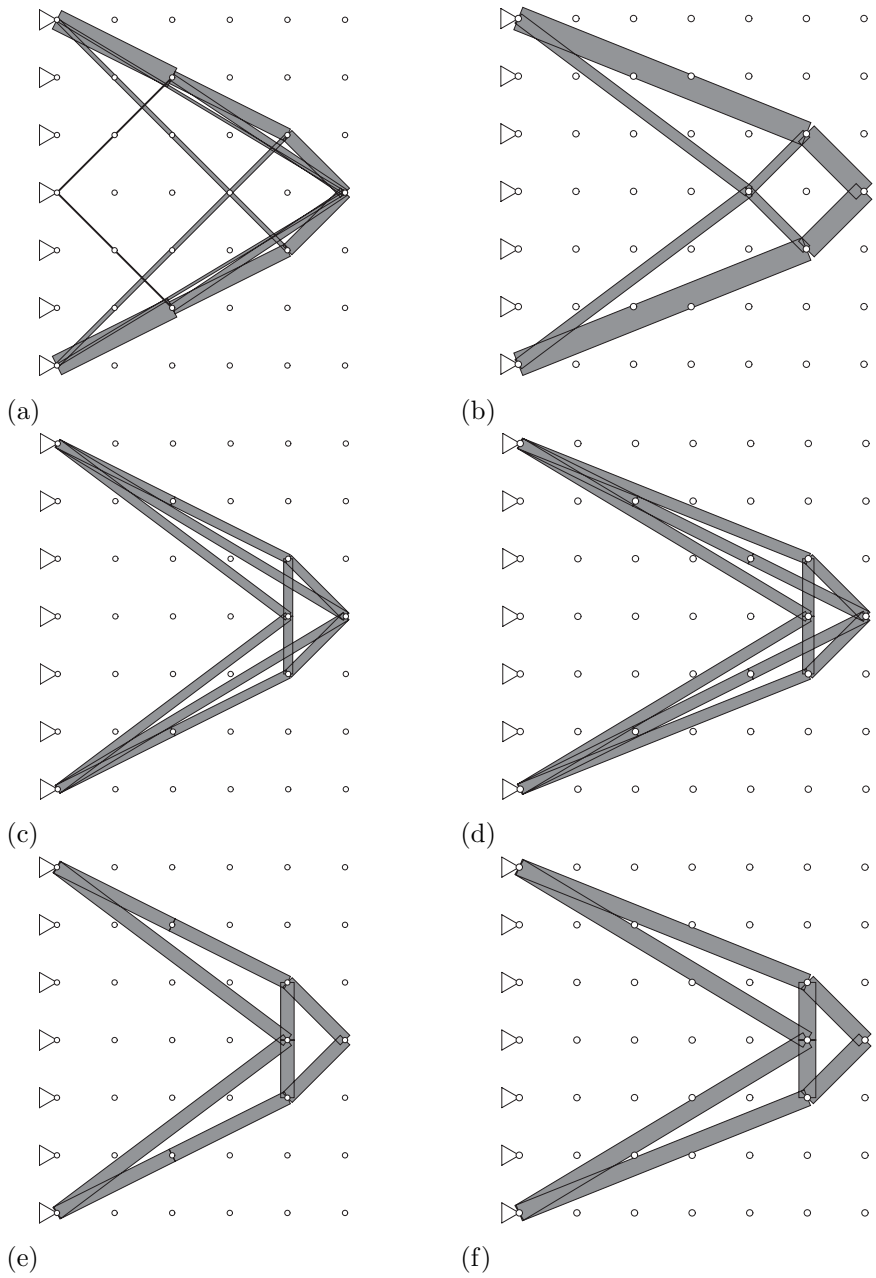

Figure 12: The optimal solutions of example (III) for $(N_X, N_Y) = (5, 6)$ and $(N_X, N_Y) = (6, 6)$. The solutions for (a) $(5, 6)$ without the standardization constraint; (b) $(6, 6)$ without the standardization constraint; (c) $(5, 6)$ with $n = 1$; (d) $(6, 6)$ with $n = 1$; (e) $(5, 6)$ with $n = 1$ and the constraints disallowing crossing members; and (f) $(6, 6)$ with $n = 1$ and the constraints disallowing crossing members.

The leftmost nodes are pin-supported. The upper bound for the member cross-sectional areas is $x^{\max} = 2000\,\mathrm{mm}^2$. The optimization results are listed in Table 6, where the column "cross. const." shows if the constraint avoiding existence of crossing members is imposed or not.

For $(N_X, N_Y) = (6, 2)$ and $(7, 2)$, the optimal solutions are collected in Figure 10. With $n = 1$, the two optimal solutions, shown in Figure 10(c) and Figure 10(d) are very similar. The increase of compliance from the continuous relaxation problem is about 5% for $(N_X, N_Y) = (6, 2)$ and more than 10% for $(N_X, N_Y) = (7, 2)$. The optimal solution for $(N_X, N_Y) = (6, 2)$ with $n = 2$ has the same topology as the optimal solution with $n = 2$. For $(N_X, N_Y) = (7, 2)$, the optimal solution with $n = 2$ has more members than that with $n = 1$. The compliance of this solution is only 2% larger than the optimal solution of the continuous relaxation problem.

For $(N_X, N_Y) = (6, 4)$ and $(7, 4)$, the optimal solutions are collected in Figure 11. For $(N_X, N_Y) = (6, 4)$, the middle node of the optimal solution of the continuous problem (in Figure 11(a)) is moved rightward in the optimal solution with $n = 1$ (in Figure 11(c)). In contrast, the optimal solution with $n = 2$ (in Figure 11(e)) is very similar to the continuous one. The optimal value for $n = 2$ is also very close to the one of the continuous optimization. For $(N_X, N_Y) = (7, 4)$, the optimal solution with $n = 1$ (in Figure 11(d)) is much different from the continuous one (in Figure 11(b)). However, the solution for $n = 2$ (in Figure 11(f)) is very similar to the continuous one. Since the solution for $n = 2$ has two pairs of mutually crossing members, we solved the problem with the constraints prohibiting presence of crossing members. The obtained solution is shown in Figure 11(g). This solution has the same topology as that in Figure 11(d), but the increase of compliance from the solution in Figure 11(f) is very small.

For $(N_X, N_Y) = (5, 6)$ and $(6, 6)$, the optimal solutions are collected in Figure 12. The optimal solutions with $n = 1$ (in Figure 12(c) and Figure 12(d)) are much different from the optimal solutions of the continuous problems (in Figure 12(a) and Figure 12(b)). Since the solutions with $n = 1$ have two pairs of mutually crossing members, we examined the constraints prohibiting the presence of crossing members. The optimal solutions are shown in Figure 12(e) and Figure 12(f). The set of existing member of each solution is a subset of that of the solution with crossing members. Nonetheless, increase of compliance is quite small.

It is observed in Table 6 that about 7 hours were required to solve the problem with $(N_X, N_Y) = (6, 6)$, which involves $m = 748$ binary variables. In contrast, the number of binary variables of the problem with $(N_X, N_Y) = (7, 4)$ and $n = 2$ is about twice, i.e., $3m = 1{,}509$, but only 17 minutes were required. The constraint prohibiting the presence of mutually crossing members is considered for $(N_X, N_Y) = (7, 4)$, $(5, 6)$, and $(6, 6)$. Compared with the case allowing crossing members, the number of enumeration nodes explored by the MISOCP solver is relatively small, although the computational time is comparably large. Prohibiting crossing members is formulated as a number of linear inequalities and this causes increase of computational time for solving a relaxation problem at each enumeration node. Indeed, 24,668 extra linear inequalities are used for $(N_X, N_Y) = (7, 4)$, 30,638 for $(5, 6)$, and 54,480 for $(6, 6)$.

6 Conclusions

Attention of this paper has been focused on finding an optimal truss design with only a limited number of different member cross-sections. It is often that the compliance optimization with continuous design variables results in a truss design with a large number of different cross-sections. Such a design may have several disadvantages from a practical point of view. The optimization method proposed in this paper simultaneously determines the groups of members which share the same cross-sections and the value of cross-sectional area used for each group.

Notion of the upper bound constraint for the number of different cross-sectional areas has been introduced. It has been shown that the compliance minimization problem with this constraint can be formulated as a mixed-integer second-order cone programming (MISOCP) problem. Several software packages are available for finding the global optimal solution of an MISOCP problem. The continuous relaxation of the proposed MISOCP problem corresponds to the conventional compliance minimization problem with continuous design variables.

The proposed method can handle the grouping constraint without resorting to any approximation. Guaranteed convergence to a global optimal solution is a distinguished attribute. Besides, this approach can deal with various kinds of practical constraints on existing members, e.g., the constraint avoiding presence of mutually crossing members.

A potential disadvantage of the method is that computational cost may possibly increase drastically as the number of variables increases. The largest ground structure solved in the numerical experiments consists of 748 members. The MISOCP solver requires about 7 hours to solve this problem when the number of different cross-sectional areas is limited to one. Also, a problem with 1600 binary variables was solved within 20 minutes. On the other hand, some smaller problems, particularly including some of multiple-load examples, require much more computational time. Distinction between time-consuming problems and easy problems is still blurred and prediction of computational cost for a particular problem is not easy. Nevertheless, it is worth noting that the proposed method can provide benchmark examples for evaluating performance of the other local or heuristic optimization algorithms.

This paper has addressed only compliance optimization of truss structures. Extensions to the other mechanical performance and the other structural models remain to be explored.

Acknowledgments

This work is partially supported by Grant-in-Aid for Scientific Research (C) 26420545 from the Japan Society for the Promotion of Science.

References

[1] Achtziger, W, Stolpe, M.: Truss topology optimization with discrete design variables—Guaranteed global optimality and benchmark examples. *Structural and Multidisciplinary Optimization*, **34**, 1–20 (2007).

[2] Alizadeh, F., Goldfarb, D.: Second-order cone programming. *Mathematical Programming*, **95**, 3–51 (2003).

[3] Allaire, G., Kohn, R.V.: Optimal design for minimum weight and compliance in plane stress using extremal microstructures. *European Journal of Mechanics A/Solids*, **12**, 839–878 (1993).

[4] Anjos, M.F., Lasserre, J.B. (eds.): *Handbook on Semidefinite, Conic and Polynomial Optimization*. Springer, New York (2012).

[5] Atamtürk, A., Narayanan, V.: Conic mixed-integer rounding cuts. *Mathematical Programming*, **122**, 1–20 (2010).

[6] Ben-Tal, A., Bendsøe, M.P.: A new method for optimal truss topology design. *SIAM Journal on Optimization*, **2**, 322–358 (1993).

[7] Ben-Tal, A., Nemirovskii, A.: Potential reduction polynomial time method for truss topology design. *SIAM Journal on Optimization*, **4**, 596–612 (1994).

[8] Bendsøe, M.P., Ben-Tal, A., Zowe, J.: Optimization methods for truss geometry and topology design. *Structural Optimization*, **7**, 141–159 (1994).

[9] Bendsøe, M.P., Haber, R.B.: The Michell layout problem as a low volume fraction limit of the perforated plate topology optimization problem: An asymptotic study. *Structural Optimization*, **6**, 263–267 (1993).

[10] Billionnet, A., Elloumi, S., Lambert, A.: Extending the QCR method to general mixed-integer programs. *Mathematical Programming*, **131**, 381–401 (2012).

[11] Bollapragada, S., Ghattas, O., Hooker, J.N.: Optimal design of truss structures by logic-based branch and cut. *Operations Research*, **49**, 42–51 (2001).

[12] Bremicker, M., Papalambros, P.Y., Loh, H.T.: Solution of mixed-discrete structural optimization problems with a new sequential linearization algorithm. *Computers and Structures*, **37**, 451–461 (1990).

[13] Cerveira, A., Agra, A., Bastos, F., Gromicho, J.: A new branch and bound method for a discrete truss topology design problem. *Computational Optimization and Applications*, **54**, 163–187 (2013).

[14] Drewes, S., Pokutt, S.: Cutting-planes for weakly-coupled 0/1 second order cone programs. *Electronic Notes in Discrete Mathematics*, **36**, 735–742 (2010).

[15] Gibiansky, L.V., Sigmund, O.: Multiphase composites with extremal bulk modulus. *Journal of the Mechanics and Physics of Solids*, **48**, 461–498 (2000).

[16] Groenwold, A.A., Stander, N.: Optimal discrete sizing of truss structures subject to buckling constraints. *Structural Optimization*, **14**, 71–80 (1997).

[17] Groenwold, A.A., Stander, N., Snyman, J.A.: A pseudo-discrete rounding method for structural optimization. *Structural Optimization*, **11**, 218–227 (1996).

[18] Gurobi Optimization, Inc.: *Gurobi Optimizer Reference Manual*. `http://www.gurobi.com/` (Accessed June 2014).

[19] IBM ILOG: *User's Manual for CPLEX*. `http://www.ilog.com/` (Accessed June 2014).

[20] Jarre, F., Kočvara, M., Zowe, J.: Optimal truss design by interior-point methods. *SIAM Journal on Optimization*, **8**, 1084–1107 (1998).

[21] Jog, C.S., Haber, R.B., Bendsøe, M.P.: Topology design with optimized, self-adaptive materials. *International Journal for Numerical Methods in Engineering*, **37**, 1323–1350 (1994).

[22] Kanno, Y.: Damper placement optimization in a shear building model with discrete design variables: A mixed-integer second-order cone programming approach. *Earthquake Engineering and Structural Dynamics*, **42**, 1657–1676 (2013).

[23] Kravanja, S., Kravanja, Z., Bedenik, B.S.: The MINLP optimization approach to structural synthesis. Part I: A general view on simultaneous topology and parameter optimization. *International Journal for Numerical Methods in Engineering*, **43**, 263–292 (1998).

[24] Lavan, O., Amir, O.: Simultaneous topology and sizing optimization of viscous dampers in seismic retrofitting of 3D irregular frame structures. *Earthquake Engineering and Structural Dynamics*, **43**, 1325–1342 (2014).

[25] Loh, H.T., Papalambros, P.Y.: A sequential linearization approach for solving mixed-discrete nonlinear design optimization problems. *Journal of Mechanical Design (ASME)*, **113**, 325–334 (1991).

[26] Makrodimopoulos, A., Bhaskar, A., Keane, A.J.: Second-order cone programming formulations for a class of problems in structural optimization. *Structural and Multidisciplinary Optimization*, **40**, 365–380 (2010).

[27] Ohsaki, M., Katoh, N.: Topology optimization of trusses with stress and local constraints on nodal stability and member intersection. *Structural and Multidisciplinary Optimization*, **29**, 190–197 (2005).

[28] Olsen, G.R., Vanderplaats, G.N.: Method for nonlinear optimization with discrete design variables. *AIAA Journal*, **27**, 1584–1589 (1989).

[29] Rasmussen, M.H., Stolpe, M.: Global optimization of discrete truss topology design problems using a parallel cut-and-branch method. *Computers and Structures*, **86**, 1527–1538 (2008).

[30] Ringertz, U.T.: A branch and bound algorithm for topology optimization of truss structures. *Engineering Optimization*, **10**, 111–124 (1986).

[31] Ringertz, U.T.: On methods for discrete structural optimization. *Engineering Optimization*, **13**, 47–64 (1988).

[32] Schmit, L.A., Fleury, C.: Discrete-continuous variable structural synthesis using dual methods. *AIAA Journal*, **18**, 1515–1524 (1980).

[33] Stegmann, J., Lund, E.: Discrete material optimization of general composite shell structures. *International Journal for Numerical Methods in Engineering*, **62**, 2009–2027 (2005).

[34] Stolpe, M.: Truss topology optimization with discrete design variables by outer approximation. *Journal of Global Optimization*, to appear. DOI: 10.1007/s10898-014-0142-x.

[35] Stolpe, M., Kawamoto, A.: Design of planar articulated mechanisms using branch and bound. *Mathematical Programming*, **103**, 357–397 (2005).

[36] Stolpe, M., Svanberg, K.: Modelling topology optimization problems as linear mixed 0–1 programs. *International Journal for Numerical Methods in Engineering*, **57**, 723–739 (2003).

[37] Templeman, A.B.: Discrete optimum structural design. *Computers and Structures*, **30**, 511–518 (1988).

[38] Vielma, J.P., Ahmed, S., Nemhauser, G.L.: A lifted linear programming branch-and-bound algorithm for mixed-integer conic quadratic programs. *INFORMS Journal on Computing*, **20**, 438–450 (2008).

[39] Yu, X., Zhang, S., Johnson, E.: A discrete post-processing method for structural optimization. *Engineering with Computers*, **19**, 213–220 (2003).

A Derivation of SOCP formulation for continuous compliance optimization

We show that problem (6) in section 2.1 can be rewritten equivalently as problem (7) in section 2.2.

By using (3) and (4), definition of the compliance in (5) can be written as

$$\pi(\boldsymbol{x}) = 2 \sup_{\boldsymbol{u},\boldsymbol{c}} \Big\{ \boldsymbol{f}^\top \boldsymbol{u} - \sum_{e=1}^{m} \frac{1}{2} \frac{E x_e}{l_e} c_e^2 \mid c_e = \boldsymbol{b}_e^\top \boldsymbol{u} \ (e = 1, \ldots, m) \Big\}. \tag{52}$$

In the following we shall derive the dual problem of the optimization problem on the right-hand side of (52). The Lagrangian of this problem can be formulated as

$$L(\boldsymbol{u}, \boldsymbol{c}; \boldsymbol{q}) = \boldsymbol{f}^\top \boldsymbol{u} - \sum_{e=1}^{m} \frac{1}{2} \frac{E x_e}{l_e} c_e^2 + \sum_{e=1}^{m} q_e (c_e - \boldsymbol{b}_e^\top \boldsymbol{u}), \tag{53}$$

with which (52) can be represented as

$$\pi(\boldsymbol{x}) = 2 \sup_{\boldsymbol{u},\boldsymbol{c}} \Big\{ \inf_{\boldsymbol{q}} \{ L(\boldsymbol{u}, \boldsymbol{c}; \boldsymbol{q}) \mid \boldsymbol{q} \in \mathbb{R}^m \} \Big\}. \tag{54}$$

It follows from the strong duality of convex quadratic programming that (54) can be replaced by the Lagrangian dual problem, i.e.,

$$\pi(\boldsymbol{x}) = 2 \inf_{\boldsymbol{q}} \Big\{ \sup_{\boldsymbol{u},\boldsymbol{c}} \{ L(\boldsymbol{u}, \boldsymbol{c}; \boldsymbol{q}) \mid (\boldsymbol{u}, \boldsymbol{c}) \in \mathbb{R}^d \times \mathbb{R}^m \} \Big\}. \tag{55}$$

By using the stationarity conditions of L with respect to $\boldsymbol{u}$ and c_e, we obtain

$$\begin{aligned}&\sup\{L(\boldsymbol{u},\boldsymbol{c};\boldsymbol{q}) \mid (\boldsymbol{u},\boldsymbol{c}) \in \mathbb{R}^d \times \mathbb{R}^m\}\\ &\quad= \begin{cases} \displaystyle\sum_{e=1}^{m} \frac{1}{2}\frac{Ex_e}{l_e}c_e^2 & \text{if } \displaystyle\sum_{e=1}^{m} q_e\boldsymbol{b}_e = \boldsymbol{f},\ q_e = \frac{Ex_e}{l_e}c_e\ (e=1,\dots,m),\\ +\infty & \text{otherwise.}\end{cases}\end{aligned} \tag{56}$$

Observe that, when $q_e = (Ex_e/l_e)c_e$ is satisfied, $x_e = 0$ implies $q_e = 0$ and

$$\frac{1}{2}\frac{Ex_e}{l_e}c_e^2 = \begin{cases} \dfrac{1}{2}\dfrac{l_e}{Ex_e}q_e^2 & \text{if } x_e > 0,\\ 0 & \text{if } x_e = 0,\end{cases}$$

and hence we can write

$$\frac{1}{2}\frac{Ex_e}{l_e}c_e^2 = \inf_{w_e}\Big\{w_e \mid w_e x_e \geq \frac{1}{2}\frac{l_e}{E}q_e^2\Big\}. \tag{57}$$

By substituting (57) into (56), we see that (55) is reduced to

$$\pi(\boldsymbol{x}) = 2\inf_{\boldsymbol{w},\boldsymbol{q}}\Big\{\sum_{e=1}^{m} w_e \mid w_e x_e \geq \frac{1}{2}\frac{l_e}{E}q_e^2\ (e=1,\dots,m),\ \sum_{e=1}^{m} q_e\boldsymbol{b}_e = \boldsymbol{f}\Big\}. \tag{58}$$

Substitution of (58) into problem (6) yields

$$\begin{aligned}
\min\quad & \sum_{e=1}^{m} 2w_e && \text{(59a)}\\
\text{s.t.}\quad & w_e x_e \geq \frac{l_e}{2E}q_e^2, \quad e=1,\dots,m, && \text{(59b)}\\
& \sum_{e=1}^{m} q_e\boldsymbol{b}_e = \boldsymbol{f}, && \text{(59c)}\\
& \sum_{e=1}^{m} l_e x_e \leq \bar{V}, && \text{(59d)}\\
& 0 \leq x_e \leq x^{\max}, \quad e=1,\dots,m, && \text{(59e)}
\end{aligned}$$

where x_e, w_e, and q_e $(e = 1,\dots,m)$ are variables to be optimized. Furthermore, the inequality constraints in (59b) can be rewritten equivalently as

$$w_e + x_e \geq \left\| \begin{bmatrix} w_e - x_e \\ \sqrt{2l_e/E}\,q_e \end{bmatrix} \right\|.$$

Thus problem (6) can be recast as problem (7).